Shallow foreshore wave height statistics

Heiko W. Groenendijk

Master's thesis
Section of Fluid Mechanics
Faculty of Civil Engineering and Geosciences
Delft University of Technology
January 1998

Abstract

Wave height distributions on shallow foreshores deviate from those in deep water due to the effects of the restricted depth-to-height ratio and of wave breaking. Laboratory data of wave heights on shallow foreshores of different slopes have been analysed to determine these effects and to derive generalised empirical parameterisation. A model distribution is proposed consisting of a Rayleigh distribution or a Weibull distribution with exponent equal to 2, for the lower heights and a Weibull with a higher exponent for the higher wave heights. The parameters of this distribution have been estimated form the data and expressed in terms of local wave energy, depth and bottom slope, yielding a predictive model that is to be significantly more accurate that existing expressions.

An abstract of this thesis is published as:

Battjes, J.A. and Groenendijk, H.W. [2000] Wave height distributions on shallow foreshores, *Coastal Engineering*, 40 (2000) 161-182

Graduation Committee:

Battjes, prof.dr.ir. J.A.
Vrijling, prof.drs.ir. J.K.
Schiereck, ir. G.J.
Van Gent, dr.ir. M.R.A.
Janssen, ir. J.P.F.M.

Acknowledgments

First of all I would like to thank my graduation committee:

Prof.dr.ir. J.A. Battjes, prof.drs.ir. J.K. Vrijling and ir. G.J. Schiereck of the Delft University of Technology, dr.ir. M.R.A. van Gent of WL | delft hydraulics and ir. J.P.F.M. Janssen of the Ministry of Transport, Public Works and Water Management (Rijkswaterstaat-DWW / WIS).

J.A. Battjes is gratefully acknowledged for his participation in the present study. His guidance was extremely motivating and resulted in the ultimate robustness of the Composed Weibull wave height distribution model. He also clearly pointed out that there is a significant difference between doing things right and doing the right things.

I would like to thank M.R.A. van Gent for revealing the relevance of wave height statistics, when my vision of the necessity of my work was obscured. Furthermore, I greatly appreciate P.K. Klok for the useful comments, suggestions and fruitful discussions about water surface elevation and all other beautiful things in life.

Finally, I would like to express my gratitude to family and friends for their support during the entire period of my study at Delft University of Technology.

Contents

1 Introduction

In order to determine loading of sea-defence works in extreme conditions knowledge of wave statistics is essential. In deep water the relatively linear and Gaussian behavior of waves allows for a theoretically sound statistical description of wave field characteristics. In shallow water the description of wave behavior is more complicated and the knowledge of the statistical description of wave field characteristics is limited. A special situation occurs when waves propagate over a shallow foreshore. The waves travel considerable distances in relatively shallow water which causes the wave characteristics to be mainly locally determined. Substantial parts of the Dutch coasts do have a shallow foreshore seaward of sea-defence works. Hence, the influence of shallow foreshores on the wave characteristics is a subject of interest to designers and authorities responsible for sea-defence works.

In this study the distribution of wave heights on shallow foreshores is investigated. The applicability of two local wave height distribution models is evaluated. These two models are the Modified Glukhovskiy distribution and a new model based on a composed Weibull distribution.

1.1 Shallow foreshore definition

A foreshore is defined as the part of the coast, seaward of a sea-defence work, which influences the wave characteristics. When the influence of the foreshore causes the distribution of wave heights to differ considerably from the Rayleigh distribution, the foreshore is called shallow. A unique definition of a shallow foreshore is not available. Pilarczyk (1996) and Van der Meer (1997) defined some shallow foreshore criteria. Some of these criteria are mentioned below as an indication and therefore should not be used as strict criteria (see also Figure 1):

1. $L_f / L_{op} > 1$

2. $\alpha < 1{:}20$

in which L_f denotes the foreshore length, L_{op} is the deep water wavelength based on the peak period T_p, α denotes the slope of the foreshore.

Criteria 1 and 2 refer to the fact that deformation of waves is a time dependent process. Waves need a certain propagation time, and therefore distance, to adapt to the changed bottom topography. A third and more important criterion is

3. $H_{1/3,t} / d_t > \frac{1}{3}$

in which $H_{1/3,t}$ is the mean of the highest 1/3-part of the wave heights at the toe of the sea-defence work and d_t is the water depth at the toe of the sea-defence work.

The third criterion results from the fact that an increasing relative wave height results in more breaking, particularly of the higher waves. When the higher waves start to break the extreme wave heights like $H_{2\%}$, $H_{1\%}$ and $H_{0.1\%}$ will decrease more than the significant wave height. This implies a deviation from the Rayleigh distribution. Gerding (1993) shows that this deviation becomes significant for wave fields of which the relative significant wave height exceeds 1/3, as indicated in Criterion 3.

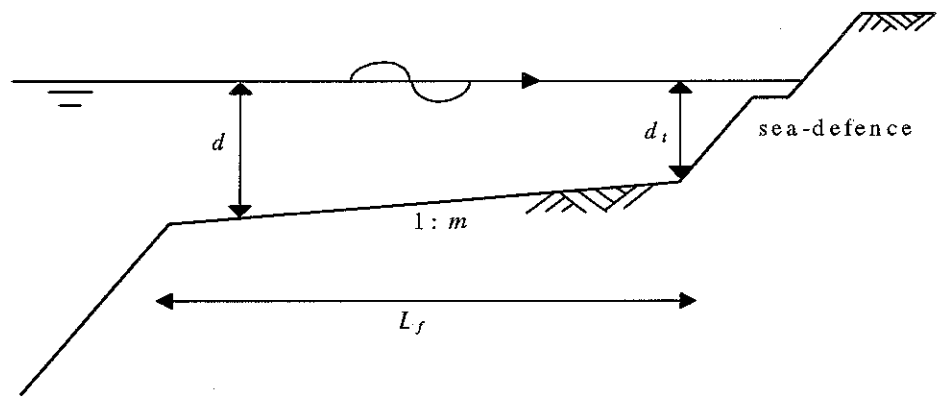

Figure 1.1: Shallow foreshore definition

1.2 Problem analysis

Design methods of sea-defence works are nowadays based on risk analysis. Therefore knowledge of wave statistics in shallow water is essential in determining design loads of sea-defence works. Most of the Dutch sea-defence works are located landward of a shallow foreshore. Since the knowledge of shallow foreshore wave statistics is limited, a problem arises when design wave heights have to be determined.

1.3 Scope and aim of this study

In this section the aim and the limitations of the present study are defined.

1.3.1 Scope

The scope of this study is limited as follows:

1. Although the wave periods and the relation of wave period to wave height are important features of the short-term wave statistics, we will focus on the distribution of individual wave heights on shallow foreshores.
2. The evaluation of shallow foreshore wave statistics using a PDF-propagation model (see Section 2.2.3) is outside the scope of this study.
3. Furthermore, in this study 2-D laboratory data are used (wave flumes). This means that only irregular waves normally incident on a foreshore with straight and parallel depth contours are considered.

1.3.2 Aim

With the scope of the study defined, the aim of this study is limited to the description of wave height distributions on shallow foreshores. To gain some insight, the deformation of a measured wave height distribution on a scale model shallow foreshore is shown below.

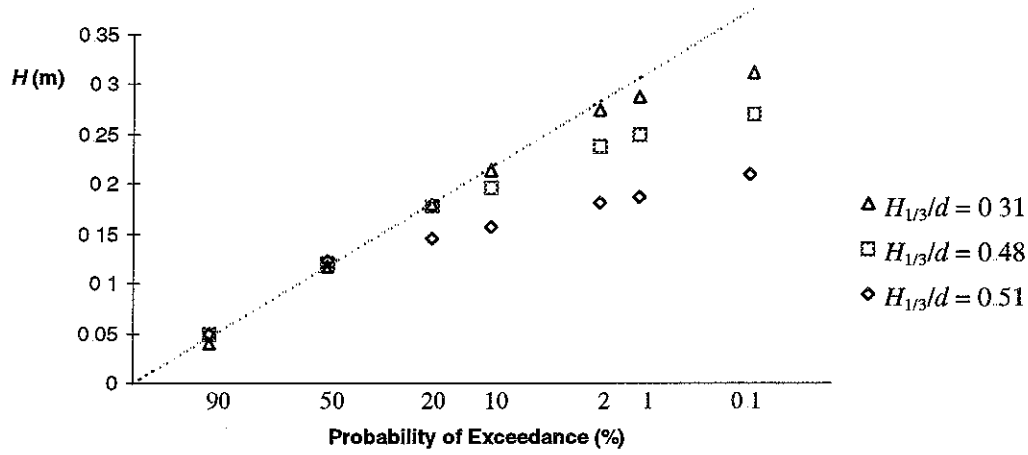

Figure 1.2: Deformation of a measured wave height distribution on a scale model shallow foreshore.

In Figure 1.2 measured wave height distributions are plotted on Rayleigh scale. The wave heights with a certain probability of exceedance are obtained from data measured at three different locations of the scale model shallow foreshore. The straight dotted line represents a Rayleigh wave height distribution. Figure 1.2 shows a deformation of the wave height distribution as the relative wave height ($H_{1/3}/d$) increases. The description of this deformation is the aim of this study. In other words:

The aim of this study is to obtain a local wave height distribution model, which uses the output of energy propagation models, suitable for describing wave height distributions on shallow foreshores.

1.4 Outline

The general outline of this report is as follows. In Chapter 2 wave modelling and wave statistics in deep and shallow water are discussed briefly. Existing local wave height distribution models are described in Section 2.3 and evaluated in Section 2.4. In Chapter 3 a composed Weibull distribution is proposed and the parameter estimation of this new distribution is described. Chapter 4 contains a description of the data used in the fit procedure and the data used to validate the proposed local wave height distribution model. In Chapter 5 the parameterisation of two parameters of the Composed Weibull distribution is carried out. In Chapter 6 the local wave height distribution model based on the Composed Weibull distribution is validated.

Although the present study by then was in a finishing stage, the author was tempted to add a seventh chapter to this report, dealing with a simpler model based on the assumption of a constant nondimensional root mean square wave height. In Chapter 8 conclusions and recommendations are presented.

2 Wave statistics

The surface elevation of sea waves is a non-stationary Gaussian process. Therefore the description of sea waves is divided into a short-term and a long-term description. Short-term refers to a time interval short enough to consider the sea state to be stationary and long enough to obtain statistically reliable results. A short-term sea state, from now on referred to as a "wave field", can be characterized by specified parameters like a significant wave height and characteristic wave period. The long-term statistical description characterizes the variability of these specified parameters, which are assumed constant in the short-term description. In this study we will focus on the short-term wave statistics.

2.1 Short-term wave statistics

The short-term wave statistics in deep water are well described. Longuet-Higgins (1952) showed that the wave heights of Gaussian waves with a narrow banded frequency spectrum obey the Rayleigh distribution:

$$F_{\underline{H}} \equiv \Pr\{\underline{H} < H\} = 1 - \exp\left[-\frac{H^2}{8m_0}\right] \tag{2.1}$$

In which m_0 is the variance of the water surface elevation. The significant wave height, $H_{1/3}$, is defined as the mean height of the highest 1/3-part of the waves in a wave field. The following expression for $H_{1/3}$ can be derived from (2.1):

$$H_{1/3} \approx 4.004\sqrt{m_0} \tag{2.2}$$

This theoretical relation is valid for wave fields with a narrow banded frequency spectrum. When real sea waves are concerned the assumption of a narrow banded frequency spectrum is violated. However, Longuet-Higgins (1980) and Tayfun (1990) proved the Rayleigh distribution to give very good approximations of measured wave height distributions in deep water. The only difference compared to (2.2) is the slightly smaller coefficient as a result of the finite frequency bandwidth occurring in windwaves:

$$H_{1/3,emp} \approx 3.8\sqrt{m_0} \tag{2.3}$$

When m_0 is eliminated from (2.1) with (2.2) the Rayleigh distribution, related to the significant wave height, is obtained:

$$Q_{\underline{H}} \equiv \Pr\{\underline{H} > H\} = \exp\left[-2\left(\frac{H}{H_{1/3}}\right)^2\right] \tag{2.4}$$

Relation 2.4 is valid regardless of the value of the coefficient in (2.2) and (2.3). With the relations mentioned above the distribution of wave heights in deep water is well described.

Rice (1954) gave an approximate distribution for the wave period, derived from wave period distributions in random noise. Longuet-Higgins (1957) presented a joint Probability Density Function (PDF) of wave height and wave period. From this joint-PDF, the PDF of

wave periods in a certain range of wave heights can be obtained, i.e. the conditional PDF of wave periods. Longuet-Higgins derived the PDF of wave periods under the assumption that the spectrum is sufficiently narrow, which is not always a theoretically correct assumption for real sea waves. However Longuet-Higgins (1975) showed his theory to be very useful in explaining the properties of wave period distributions. He proved that the agreement between theory and measurements is reasonably good for waves propagating in deep water.

In shallow water the situation changes considerably. When the relative wave height increases, processes like depth-induced breaking, shoaling, triad interactions and bottom friction become relevant. Triad interactions and depth-induced breaking in particular are manifestations of strongly nonlinear behavior of waves, resulting in nonlinear spectral components and a strong increase of spectral width. The limited depth also causes the waves to have a definite excess of crest heights and shallow troughs, in contrast to the Gaussian waves in deep water.

Thus, the surface elevation in shallow water can no longer be considered a narrow banded linear Gaussian process. This poses a problem for the description of wave statistics in shallow water, since the wave statistics rely heavily on the assumption of a sufficiently narrow banded, linear and Gaussian surface elevation. So instead of the theoretically sound Rayleigh distribution and joint distribution of wave height and wave period, other methods of describing the wave statistics in shallow water are to be used.

2.2 Shallow water wave modelling and wave statistics

In the description of wave characteristics, numerical wave modelling is of great importance. In the last decade several numerical wave models, evaluating wave evolution in the nearshore region, have been developed. Battjes (1994) roughly divided these numerical wave models into phase-resolving models and phase-averaged models.

The phase-resolving models are based on equations describing the instantaneous state of motion. These models are to be applied in situations where the phase-averaged properties vary strongly within distances of the order of a wavelength or less.

In contrast, phase-averaged models are used when the variations of the wave properties are weak on the scale of a wavelength. The phase-averaged models are able to describe wave behaviour over large areas, using energy balance and kinematic propagation equations.

Phase-resolving and phase-averaged models yield information from which wave height distributions can be constructed. However, the fundamental difference between phase-resolving and phase-averaged models results in different approaches for obtaining wave height probability density functions.

2.2.1 Phase-resolving

When using a phase-resolving model, for instance based on fully non-linear, non-dispersive shallow water wave equations (e.g. ODIFLOCS), weakly non-linear, weakly dispersive shallow water equations (Boussinesq models) or the full Navier-Stokes equations (e.g. SKYLLA), the following procedure could yield a wave height PDF at any location seaward of a sea-defence work:

- A deep water wave field, of which the waves obey the Rayleigh distribution, is generated.
- The propagation and deformation of the waves in the wave field is evaluated with a phase-resolving model.

- At the location of concern the waves are registered and from the deformed waves a wave height distribution can be constructed.

Phase-resolving wave models are suitable for the description of waves in the nearshore region. The state-of-the-art phase-resolving models are able to give a physically sound description of complex processes, like depth-induced breaking. However, two drawbacks of using phase-resolving wave models must be noted:

• In phase-resolving modelling the spatial resolution has to be very high. In order to construct a reliable wave height distribution at least 500 waves have to be propagated from relatively deep water to the location of concern. Therefore a lot of computation time is needed to yield a reliable wave height distribution.

• Models based on non-linear, non-dispersive shallow water wave equations, like ODIFLOCS, can yield relatively accurate predictions for strongly non-linear processes. Waves, breaking on a breakwater, are reasonably well described by non-linear shallow water equations, since this wave breaking process is strongly non-linear. However, for dispersive waves the non-linear, non-dispersive shallow water wave equations often yield too much wave breaking. This may result in an overestimation of the wave energy dissipation. This problem increases with an increasing traveling distance of the waves.

2.2.2 Phase-averaged

A phase-averaged wave (energy) propagation model can yield the wave energy frequency/direction spectrum at any location seaward of a sea-defence work. However one issue becomes relevant when a phase-averaged model is used to obtain a wave height distribution in extreme shallow water.

In shallow water the surface elevation can no longer be assumed to be a narrow banded, linear and Gaussian process. When the effects of nonlinearities and the non-Gaussian behaviour of the waves are accounted for in the energy balance and propagation equations, still a problem exists in determining a wave height distribution from the results yielded by a phase-averaged model. In deep water a wave height distribution is determined by the surface elevation variance, m_0, or a characteristic wave height, like the significant wave height. In shallow water the wave heights no longer obey the Rayleigh distribution. Therefore additional information about the distribution of the wave heights, must be available in order to construct a wave height distribution.

2.2.3 PDF-propagation models

Although the wave propagation models mentioned above have been developed to evaluate the evolution of waves in the nearshore region, these models are not suitable for obtaining wave height distributions in shallow water. The phase-resolving models take too much time to evaluated a sufficiently large number of waves. The phase-averaged models yield phase-averaged wave properties but not a wave height distribution. Therefore a necessity exists for additional models, describing the individual wave heights in shallow water.

There are two types of models for the description of individual wave heights in shallow water, i.e. Probability Density Distribution propagation models (PDF-propagation models) and local wave height distribution models (pointmodels).

The PDF-propagation models describe the wave height distribution as a function of the distance from the coastline. PDF-propagation models consider the irregular wave field to be a sum of several classes of regular waves with a certain frequency of occurrence. These

classes of regular waves are considered to propagate independently over the foreshore to the coastline and the propagation of every class is evaluated with a wave energy propagation model. In doing so a certain deep water wave height PDF is propagated over a foreshore to the coast, while transforming. The deep water wave height PDF can be described with a Rayleigh distribution or a PDF determined from a local wave height distribution model for deep water. However, as mentioned in Section 1.3, the evaluation of shallow foreshore wave statistics with a PDF-propagation model is outside the scope of this study.

2.3 Local wave height distribution models

The philosophy behind local wave height distribution models is based on the assumption that the wave height distribution is mainly determined by the local parameters of the wave field and the water depth regardless of the history of the waves in deeper water. This assumption proves to be valid for shallow water with a reasonably simple bottom topography.

Few local wave height distribution models are available for shallow water. In this section the following shallow water wave height distributions are described:

- Glukhovskiy distribution
- Modified Glukhovskiy
- New Modified Glukhovskiy
- Split-Weibull distribution

In Section 2.4 a semi-quantitative evaluation is carried out to gain some insight in the applicability of these local wave height distribution models on shallow foreshores.

2.3.1 Glukhovskiy distribution

In 1966 Glukhovskiy proposed a shallow water wave height distribution, based on a two parameter Weibull distribution. These two parameters were empirically modelled as a function of the mean local wave height to local water depth ratio, H_m/d. The cumulative distribution function is:

$$F_{\underline{H}}(H) \equiv \Pr\{\underline{H} \le H\} = 1-\exp\left(-\frac{\pi}{4}A\left(\frac{H}{H_m}\right)^{\kappa}\right) \tag{2.5}$$

with

$$\kappa = \frac{2}{1-\tilde{d}}, \tag{2.6}$$

$$A = \left(1+\frac{\tilde{d}}{\sqrt{2\pi}}\right)^{-1} \tag{2.7}$$

and

$$\tilde{d} = \frac{H_m}{d} \tag{2.8}$$

In deep water this distribution reduces to the Rayleigh distribution.

2.3.2 Modified Glukhovskiy distribution

In 1986 Battjes pointed out an internal inconsistency of the Glukhovskiy distribution. He pointed out that given the following distribution:

$$F_{\underline{H}}(H) \equiv \Pr\{\underline{H} \le H\} = 1 - \exp\left(-A\left(\frac{H}{H_m}\right)^{\kappa}\right) \tag{2.9}$$

only one of the two parameters κ and A can be chosen freely. If κ is chosen according to (2.6), then A is determined as follows. Since H_m is defined as the expectation of the wave height:

$$H_m = E\{\underline{H}\} = m_1 \tag{2.10}$$

the equation for the n^{th} moment of the "Modified Glukhovskiy distribution" reads:

$$m_n = H_m^n A^{-\frac{n}{\kappa}} \Gamma\left(\frac{n}{\kappa}+1\right) \tag{2.11}$$

Therefore

$$m_1 = H_m A^{-\frac{1}{\kappa}} \Gamma\left(\frac{1}{\kappa}+1\right) \tag{2.12}$$

To assure consistency, the first moment of the Modified Glukhovskiy distribution must equal the mean H_m, yielding:

$$A = \left[\Gamma\left(\frac{1}{\kappa}+1\right)\right]^{\kappa} \tag{2.13}$$

The Modified Glukhovskiy distribution reduces to a Rayleigh distribution in deep water:

$$d \to \infty \Rightarrow \tilde{d} = \frac{H_m}{d} \to 0 \Rightarrow \kappa = \frac{2}{1-\tilde{d}} \to 2 \Rightarrow A \to \left[\Gamma\left(\frac{3}{2}\right)\right]^2 = \frac{\pi}{4} \tag{2.14}$$

Klopman and Stive (1989) have used the Modified Glukhovskiy distribution (2.9), in which A is determined by Equation 2.13 to ensure consistency and κ denotes the exponent as proposed by Glukhovskiy (2.6).

2.3.3 New Modified Glukhovskiy

The Modified Glukhovskiy distribution, though now consistent, gives a non-conservative prediction of the extreme wave heights. Therefore Klopman (1996) proposed a more conservative distribution:

$$F_{\underline{H}}(H) \equiv \Pr\{\underline{H} \le H\} = 1 - \exp\left(-A\left(\frac{H}{H_{rms}}\right)^{\kappa^*}\right) \tag{2.15}$$

In this distribution Klopman introduces an exponent κ^*, which is assumed to be a function of the relative wave height parameter d^*:

$$d^* = \frac{H_{rms}}{d} \tag{2.16}$$

The exponent κ^* differs from the original exponent since a coefficient β is added to assure conservatism:

$$\kappa^* = \frac{2}{1-\beta d^*} \tag{2.17}$$

Another difference compared to the "old" Modified Glukhovskiy distribution is the normalized wave height H/H_{rms}. In this normalized wave height the root mean square wave height is used instead of the mean wave height proposed by Glukhovskiy in 1966. Klopman relates this root mean square wave height to the variance of the water surface elevation m_0. This provides a relation between the output of wave energy propagation models and the individual wave height distribution. Klopman assumes the relation between H_{rms} and m_0 to be as in the Rayleigh distribution of a narrow banded process:

$$H_{m_0} = 4\sqrt{m_0} = \sqrt{2}\, H_{rms} \tag{2.18}$$

The n^{th} moment of this "New Modified Glukhovskiy distribution" is:

$$m_n = (H_{rms})^n A^{-\frac{n}{\kappa^*}} \Gamma\left(\frac{n}{\kappa^*}+1\right) \tag{2.19}$$

To assure consistency for this New Modified Glukhovskiy distribution m_2 has to equal $(H_{rms})^2$. This yields the following relation between the coefficient A and κ^*:

$$A = \left[\Gamma\left(\frac{2}{\kappa^*}+1\right)\right]^{\frac{\kappa^*}{2}} \tag{2.20}$$

The coefficient β in equation (2.17) has been fitted to the laboratory data sets used in 1989 by Klopman and Stive. $\beta = 0.7$ gives a good approximation of measured wave heights (Klopman 1996). This New Modified Glukhovskiy distribution yields a consistent and conservative wave height distribution which is (empirically) related to the output of wave energy propagation models via m_0.

2.3.4 Split Weibull distribution

In 1993 Van Vledder proposed a distribution with a variable shape parameter $\kappa(H)$, which varies continuously between κ_1 and $\kappa_1+\kappa_2$, called the Split Weibull distribution. The cumulative probability function is:

$$F_{\underline{H}}(H) \equiv \{\underline{H} \le H\} = 1 - \exp\left(-\left(\frac{H}{\sigma}\right)^{\kappa(H)}\right) \tag{2.21}$$

in which H denotes the wave height, σ is a scale factor and $\kappa(H)$ is a variable shape parameter. The shape parameter equals a constant κ_1 for small wave heights. For wave heights near and above a transition point, H_t, the shape parameter tends to the constant value $\kappa_1+\kappa_2$. The change in shape parameter is assumed to be given by:

$$\kappa(H) = \kappa_1 + \kappa_2 \exp\left(-\left(\frac{H_t}{H}\right)^n\right) \qquad (2.22)$$

The dependence of $k(H)$ on a transition exponent n is illustrated in Figure 2.1.

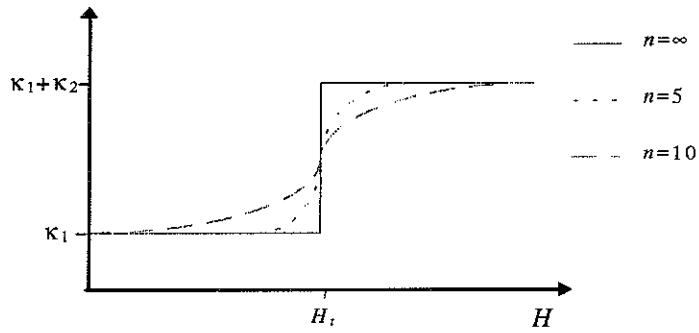

***Figure 2.1** Shape parameter $\kappa(H)$ and the influence of the transition zone exponent n.*

The idea behind this Split Weibull distribution is that measured shallow foreshore wave height distributions are better approximated by a distribution with a variable shape parameter (see also Figure 1.2).

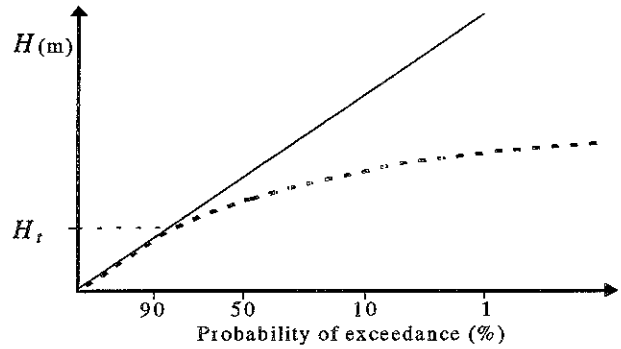

***Figure 2.2** Split Weibull distribution (dotted line) presented on Rayleigh scale*

Figure 2.2 shows a Rayleigh and a Split Weibull wave height distribution, presented on a Rayleigh scale. The straight solid line represents a Rayleigh distribution. The dotted line represents the Split Weibull distribution with a Rayleigh shape for small wave heights and a different shape for large wave heights.

The Split Weibull probability density function is determined by differentiation of the cumulative probability function (2.21). Van Vledder (personal communication 1997) poses the following Split Weibull probability density function:

$$f(H) = \frac{1}{H}\left(\frac{H}{\sigma}\right)^{\kappa(H)} \exp\left[-\left(\frac{H}{\sigma}\right)^{\kappa(H)}\right]\left\{n\kappa_2\left(\frac{H_t}{H}\right)^n \ln\left(\frac{H}{\sigma}\right)\exp\left[\left(-\frac{H_t}{H}\right)^n\right] + \kappa(H)\right\} \qquad (2.23)$$

With (2.22) Equation 2.23 is rewritten into:

$$f(H) = \left(\frac{H}{\sigma}\right)^{\kappa(H)} \exp\left[-\left(\frac{H}{\sigma}\right)^{\kappa(H)}\right]\left(\frac{d\kappa(H)}{dH}\ln\left(\frac{H}{\sigma}\right)+\frac{\kappa(H)}{H}\right) \qquad (2.24)$$

Note: In the appendix A of Klopman (1995) an incomplete version of Van Vledder (1993) is used. In the incomplete version of Van Vledder (1993) the probability density function is defined as $f(H)=H^{-1}$.

2.4 Evaluation of existing wave height distribution models

The aim of this study, as described in Section 1.3, is to find a suitable model for the description of the wave heights on shallow foreshores. Therefore a semi-quantitative evaluation of the Rayleigh distribution, the Modified Glukhovskiy distribution and the New Modified Glukhovskiy distribution is carried out. Figure 2.3 shows a typical shallow foreshore wave height distribution.

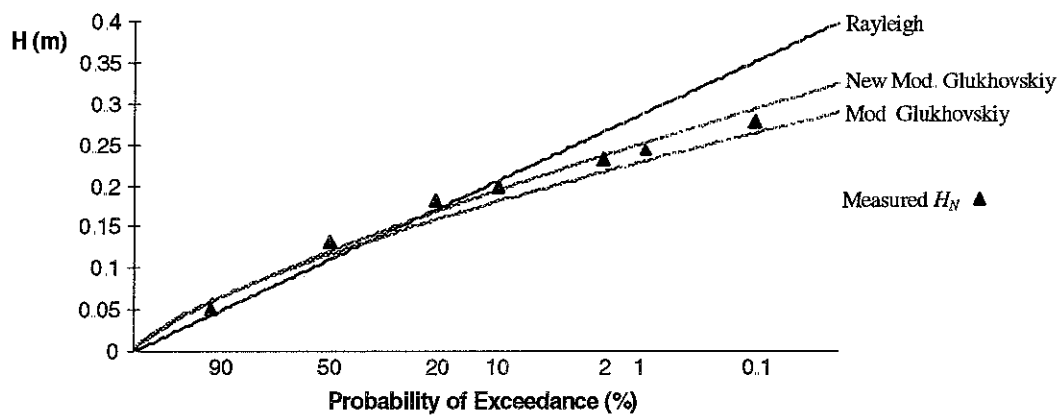

Figure 2.3: Comparison of existing models to measured shallow foreshore wave heights with a certain probability of exceedance.

This particular graph shows a wave height distribution, measured in a wave flume with a scale model shallow foreshore. The local significant wave height to local water depth ratio, $H_{1/3}/d$, equals 0.47. The foreshore slope is 1:100. For comparison the Rayleigh distribution, the Modified Glukhovskiy distribution and the New Modified Glukhovskiy distribution are plotted in Figure 2.3. The wave height distributions are calculated with the measured water surface elevation variance $m_0 = 2.26*10^{-3}$ m^2 and water depth $d = 0.41$ m.

Figure 2.3 shows that the New Modified Glukhovskiy distribution gives a relatively good overall prediction approximation of the measured wave heights. However, this distribution overestimates the extreme wave heights. Therefore Klopman (1995) states that a Split-Weibull distribution, as proposed by Van Vledder (1993), is in principle able to give the best approximation of measured wave height distributions on a shallow foreshore.

The following drawbacks of the Split Weibull distribution must be noted:

1. The fact that this distribution has five independent parameters (σ, H_t, n, κ_1 and κ_2) makes an estimation of their values very difficult, and causes the model to suffer from lack of robustness.

2. The value of the transition zone exponent, n, in the exponent $\kappa(x)$, which determines the width of the transition zone between κ_1 and $\kappa_1 + \kappa_2$, is difficult to estimate It is questionable whether or not a trustworthy value can be determined.

Therefore a composed distribution with fewer independent parameters is proposed, hopefully yielding a useful description of individual wave heights on shallow foreshores It will be described hereafter.

3 Proposed wave height distribution

Van Vledder (1993) proposed a Split Weibull distribution with a variable shape parameter, which depends on a transition zone parameter. The transition zone parameter provides a gradual change of the shape parameter from κ_1 to $\kappa_1+\kappa_2$, as described in Section 2.3.4. However, here the change in shape parameter is assumed discontinuous. Therefore the following discontinuous exponent $\kappa(H)$ is proposed:

$$\kappa(H) \equiv \begin{cases} const. = k_1 & H \le H_{tr} \\ const. = k_2 & H > H_{tr} \end{cases} \tag{3.1}$$

in which H_{tr} denotes a transitional wave height.

3.1 Composed Weibull distribution

With the discontinuous shape parameter $\kappa(H)$ the wave height distribution is composed of two separate Weibull distributions. Two different exponents k_1 and k_2 determine the shape of the distributions and two scale parameters, H_1 and H_2, are used to scale the distributions to the wave heights of concern. The composed wave height distribution is valid for $0 < H < \infty$. This domain is split in two by the transitional wave height, yielding the following composed cumulative probability function:

$$F(H) \equiv \Pr\{\underline{H} \le H\} = \begin{cases} F_1(H) = 1 - \exp\left[-\left(\dfrac{H}{H_1}\right)^{k_1}\right] & H \le H_{tr} \\ F_2(H) = 1 - \exp\left[-\left(\dfrac{H}{H_2}\right)^{k_2}\right] & H > H_{tr} \end{cases} \tag{3.2}$$

In order to obtain a continuous distribution the Composed Weibull distribution must satisfy the following condition:

$$F_1(H_{tr}) = F_2(H_{tr}) \tag{3.3}$$

Superposition of (3.2) in (3.3) yields:

$$\left(\frac{H_{tr}}{H_1}\right)^{k_1} = \left(\frac{H_{tr}}{H_2}\right)^{k_2} \tag{3.4}$$

The continuity condition causes one of the five parameters of the Composed Weibull distribution to be dependent, reducing the number of independent parameters to four. Hereafter, independent parameter refers to a parameter which is not constrained by an assumption about its value or its dependence on other parameters of the Composed Weibull distribution.

In Figure 3.1 the Composed Weibull distribution is presented on Rayleigh scale.

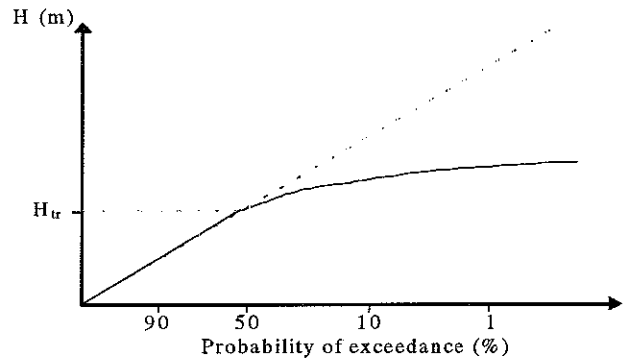

Figure 3.1 Proposed wave height distribution: The Composed Weibull distribution

Differentiation of the cumulative probability function with respect to the wave height H yields the probability density function:

$$f(H) = \frac{d\,F(H)}{dH} = \begin{cases} f_1(H) = \dfrac{k_1}{H_1^{k_1}}\, H^{k_1-1} \exp\left[-\left(\dfrac{H}{H_1}\right)^{k_1}\right] & H \le H_{tr} \\ f_2(H) = \dfrac{k_2}{H_2^{k_2}}\, H^{k_2-1} \exp\left[-\left(\dfrac{H}{H_2}\right)^{k_2}\right] & H > H_{tr} \end{cases} \tag{3.5}$$

3.2 Mean of the highest 1/N-part

In coastal engineering the mean of the highest $1/N$-part of the wave heights in a wave field is often used to characterise that wave field ($N \ge 1$). A derivation of $H_{1/N}$ of the Composed Weibull distribution is presented in Appendix A. In this section the results are presented to obtain some insight in the behaviour of the Composed Weibull distribution. $H_{1/N}$ is defined by:

$$H_{1/N} = \frac{\int_{H_N}^{\infty} H\, f(H)\,dH}{\int_{H_N}^{\infty} f(H)\,dH} = \frac{\int_{H_N}^{\infty} H\, f(H)\,dH}{\frac{1}{N}\int_{0}^{\infty} f(H)\,dH} = N \int_{H_N}^{\infty} H\, f(H)\,dH \tag{3.6}$$

In this definition H_N is the wave height with an exceedance probability of $1/N$ ($N \ge 1$). H_N is determined by evaluating the cumulative density distribution. In this case the distribution is a composition of two separate distributions. Therefore the determination of $H_{1/N}$ depends on the fact whether or not H_N exceeds H_{tr}.

If only the higher waves break and therefore deviate from the Rayleigh distribution, the transitional wave height may exceed the wave height with the given exceedance probability of $1/N$. This case is shown in Figure 3.2. When $H_{tr} > H_N$, $H_{1/N}$ of the Composed Weibull distribution is (see Appendix A.1):

$$H_{1/N} = N \int_{H_N}^{H_{tr}} H\, f_1(H)\,dH + N \int_{H_{tr}}^{\infty} H\, f_2(H)\,dH \tag{3.7}$$

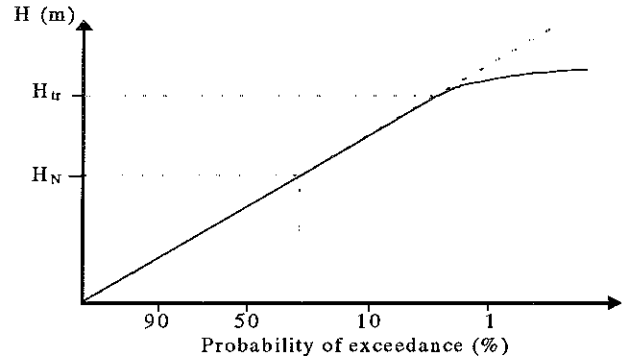

Figure 3.2: Composed Weibull wave height distribution with $H_{tr}>H_N$

With the transformation and the incomplete gamma functions, described in Appendix A.1, Equation 3.5 yields:

$$H_{1/N} = NH_1\left(\Gamma\left[\frac{1}{k_1}+1,\ \ln(N)\right]-\Gamma\left[\frac{1}{k_1}+1,\ \left(\frac{H_{tr}}{H_1}\right)^{k_1}\right]\right) + NH_2\Gamma\left[\frac{1}{k_2}+1,\ \left(\frac{H_{tr}}{H_2}\right)^{k_2}\right] \quad (3.8)$$

Figure 3.3 shows a wave height distribution on a shallow foreshore for the case $H_{tr}<H_N$.

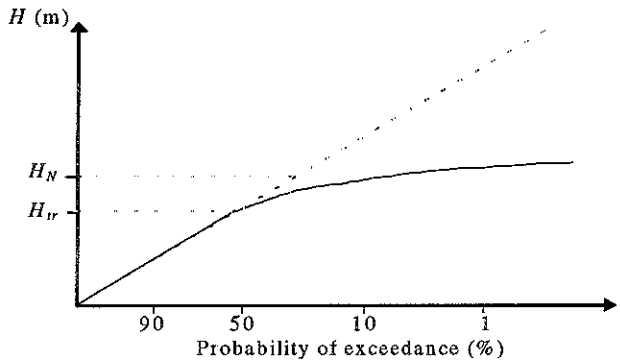

Figure 3.3: Composed Weibull wave height distribution with $H_{tr}<H_N$

The $H_{1/N}$ of the Composed Weibull distribution when $H_{tr}<H_N$ is (see Appendix A.1):

$$H_{1/N} = N\int_{H_N}^{\infty} H\, f_2(H)\, dH \quad (3.9)$$

With the transformation and incomplete gamma functions, described in Appendix A.1, Equation 3.9 yields:

$$H_{1/N} = N\,H_2\Gamma\left[\frac{1}{k_2}+1,\ \ln(N)\right] \quad (3.10)$$

In coastal engineering design practice one is often interested in the ratio of an extreme wave height to the significant wave height, $H_{2\%}/H_{1/3}$, $H_{1\%}/H_{1/3}$ or $H_{0.1\%}/H_{1/3}$. Expressions for these ratios are derived in Appendix A.2.

3.3 Parameter estimation

In this section the parameters of the Composed Weibull distribution are described.

3.3.1 Degree of saturation

The proposed distribution, as described in Section 3.1, has four independent parameters. Hence, in order to describe the measured wave height distribution of a certain wave field, the four independent parameters of the Composed Weibull distribution have to be obtained from that wave field. The properties of the nondimensional wave height distribution are assumed to be characterized by a relative local wave height, such as $H_{1/3}/d$. However, in order to relate the four independent parameters of the Composed Weibull distribution to the output of an energy propagation model a different relative wave height has to be used. This is because in shallow water the significant wave height $H_{1/3}$ is no longer uniquely related to the spectral wave height H_{m0}. Therefore instead of $H_{1/3}/d$ another degree of saturation is used to characterise the wave deformation process on shallow foreshores:

$$\Psi = \frac{\sqrt{m_0}}{d} \tag{3.11}$$

in which m_0 is the variance of the water surface elevation, which equals the zero-th spectral moment and d denotes the water depth.

3.3.2 Limiting of estimation parameters

When the independent parameters of the Composed Weibull distribution can be related to the degree of saturation, Ψ, the local wave height distribution can be obtained from the output of an energy propagation model. In order to relate the parameters of the Composed Weibull distribution to the degree of saturation the parameters must be estimated by fitting the proposed distribution to several measured wave height distributions for different degrees of saturation. It is desirable to limit the number of independent parameters as much as possible. In order to decrease the number of independent parameters assumptions about the exponents of the Composed Weibull distribution are proposed.

The first assumption comes forth from an initial inspection of measured wave height distributions. Measured wave height distributions plotted on Rayleigh scale show a straight line for the lower wave heights. Therefore it is assumed that the first part of the Composed wave height distribution, $F_1(H)$, is Rayleigh shaped. This means that the exponent k_1 equals the exponent of the Rayleigh distribution ($k_1 = 2$).

Initial visual fitting of the Composed Weibull distribution to measured wave height distributions yielded a relation between exponent k_2 and the degree of saturation as presented in Figure 3.4. It shows a decrease of the scatter in k_2 as the degree of saturation increases. High scatter for low Ψ-values is understandable. When the Composed Weibull distribution is fitted to measured wave height distribution of wave fields with low degrees of saturation the distribution hardly deviates from the Rayleigh distribution. This results in fitting of the second part of the Composed Weibull distribution to only a few measured wave heights with a low probability of exceedance. This explains the scatter for low Ψ-values. At the same time, it implies that the value of k_2 is not important for low Ψ-values.

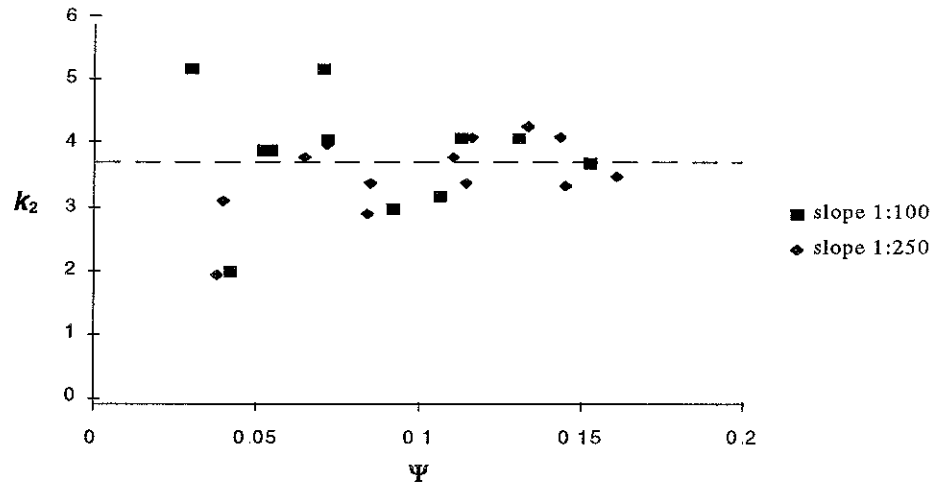

Figure 3.4: Exponent k_2 versus degree of saturation in initial fitting procedure. Calibration data

Since the higher degrees of saturation represent the area of interest, Figure 3.4 supports an assumption of a constant exponent k_2. A first guess $k_2 = 3.75$ seemed reasonable. However, after completion of the fit procedure for 20 tests k_2 was decreased and again the Composed Weibull distribution was fitted to the measured wave height distributions. An exponent k_2=3.5 yielded a better overall approximation of the measurements. This better approximation compared to $k_2 = 3.75$ is based on visual inspection of fitted distributions. Therefore an optimum value for k_2 will probably not equal 3.5. Since the determination of this optimum is time consuming, for now $k_2 = 3.5$ is used.

With these assumptions two independent parameters remain for which a reasonably straightforward fitting procedure can be defined.

3.3.3 Fit procedure

The aim of the fit procedure is to obtain an optimal fit of the composed distribution to a measured wave height distribution, by estimating the independent parameters. With the continuity condition (3.3) and the assumptions, mentioned above, only two independent parameters have to be estimated, namely two of the three characteristic wave heights (H_1, H_2 and H_{tr}).

In Figure 3.5 a measured wave height distribution is presented on Rayleigh scale.

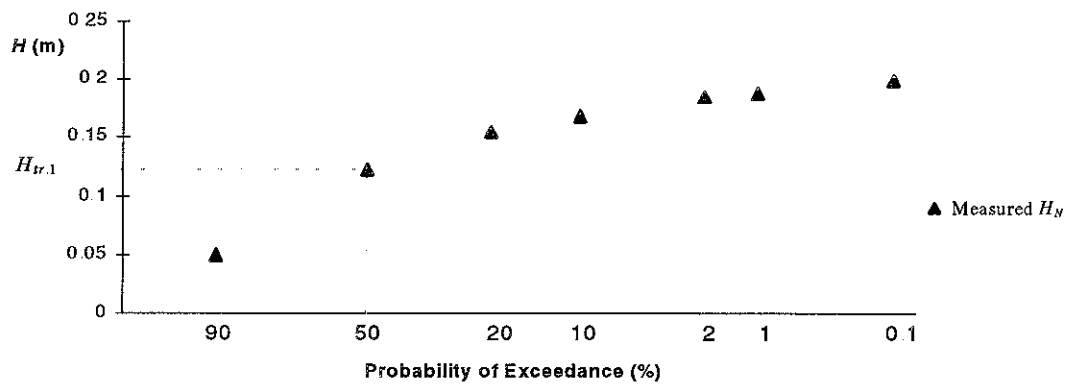

Figure 3.5: Measured shallow foreshore wave height distribution

With this measured wave height distribution as an example the estimation procedure is described as follows:

1. A clear change in the trend of measured wave heights is observed. A first (visual) estimate is made of the wave height at which the trend changes. This first estimation of the transitional wave height, H_{tr}, is presented in Figure 3.5 as $H_{tr,1}$. (In this example, it happens to be the wave height exceeded by about fifty percent of the waves, $H_{50\%}$)
2. A straight line is fitted through the measured wave heights smaller than $H_{tr,1}$. This straight line represents the first part of the Composed Weibull distribution $F_1(H)$. A least squares optimisation method yields a first estimate for H_1.
3. A first estimate of H_2 is made using Equation 3.4, for estimated values of H_{tr} and H_1 and assumed exponents (k_1=2 and k_2=3.5).
4. Using the first estimate of H_2 the distribution $F_2(H)$ is fitted to the upper part of the wave data, using a least squares optimisation method. This yields a second estimate of H_2.
5. Step 4 yields a new estimate of H_2, which probably deviates from the first estimate of H_2. Therefore steps 1 to 4 are repeated until a match with prescribed accuracy is achieved between H_2, obtained in step 3 and H_2, obtained in step 4. This results in the final estimates of H_1, H_2 and H_{tr}.

As an example, Figure 3.6 shows the result of this procedure, applied to the same measured wave height distribution as in Figure 3.4.

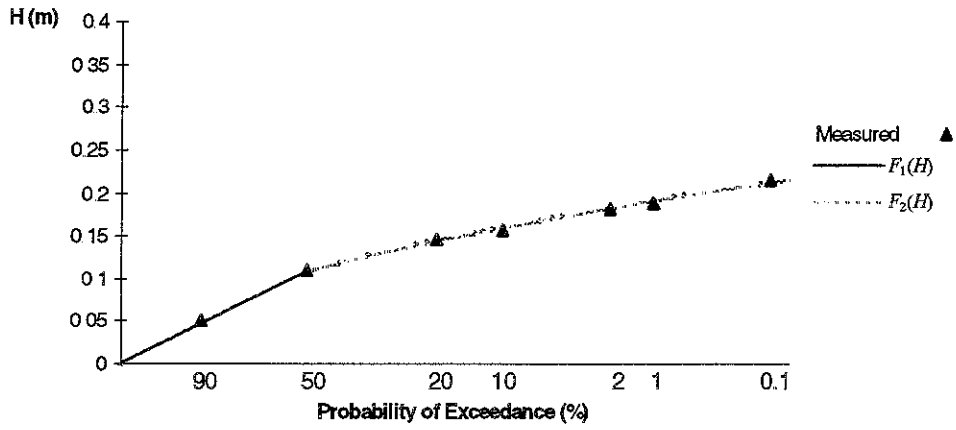

Figure 3.6: $F_1(H)$ and $F_2(H)$ fitted to a measured wave height distribution. Calibration data.

4 Data

4.1 Available data

In order to relate the parameters of the Composed Weibull distribution to the degree of saturation, measured wave height distributions, corresponding local water depths and corresponding zero-th spectral moments are necessary. The available shallow foreshore data, obtained from tests executed by WL | delft hydraulics, are presented in Table 4.1.

Table 4.1 Available shallow foreshore wave flume data

Slope	project	Number of tests	Number of gauges	Range of $H_{1/3}/d$	Range of $H_{1/3}/H_{1/3,0}$	Range of sqrt(m_0)/d	Range of s_{op}	Number of waves
1:20	H1874 Gerding '93	22	4	0.16 - 0.83	1.1 - 0.75	0.044 - 0.137	0.01 - 0.04	1000
1:50	H1874/50 Gerding '93	16	4	0.14 - 0.65	1.1 - 0.72	0.035 - 0.154	0.017 - 0.04	200
1:100	H1256 Van der Meer '93	17	18	0.13 - 0.6	1.1 - 0.51	0.04 - 0.16	0.01 - 0.04	1100
1:250	H0462.25 Van der Meer '88	72	19	0.11 - 0.6	1.15 - 0.35	0.03 - 0.15	0.008 - 0.03	1000

All tests were executed in the wave flume "Scheldegoot". In the following section the wave flume and the test set-up are described.

4.2 Wave flume "Scheldegoot"

The "Scheldegoot" is a wave flume with a wave maker capable of generating both periodic and random waves. The wave generator is equipped with a device that absorbs incoming wave energy and so prevents reflection against the wave board and avoids undesired long-periodical waves. At the back of the wave flume a spending beach provides wave damping. The wave maker's control signal is a digitized time series.

The length of this wave flume is 50 m, the width 1.0 m and the depth 1.2 m. An overview of a test set-up of a shallow foreshore with slope 1:100 is given in Figure 4.1. Other test set-ups are presented in Appendix B.

During a test a number of waves is generated by the wave board at the beginning of the wave flume. Wave gauges are placed along the shallow foreshore to measure the surface elevation at different mean water depths. The mean water depth, d, refers to the still water depth. From the measured surface elevation at different water depths statistical wave heights (like $H_{1/3}$, H_{rms} etc.), wave height distributions and spectral moments are determined.

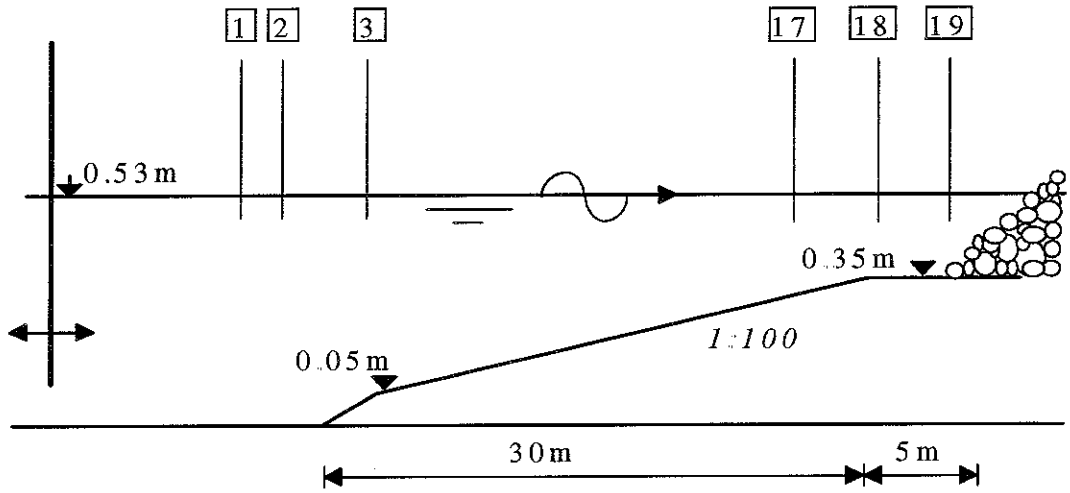

Figure 4.1 Test set-up.

4.3 Data selection

The behaviour of waves on steeper slopes deviates from the behaviour on the gentle slopes. Since the influence of the foreshore slope is not taken into account in the present study, we focus on the gentle slopes (1:100 and 1:250). From the available data on the gentle slopes two sets of data are selected. First a set of tests is selected to calibrate the Composed Weibull distribution and to obtain parameterisations for the scale wave height H_1 and the transitional wave height H_{tr}. The data are selected to represent the entire range of relative wave heights. These so called calibration data are shown in Table 4.2.

Table 4.2 Calibration data ($\overline{H_{1/3} / d} = 0.411$).

local $H_{1/3}/d$	0 - 0.1	0.1 - 0.2	0.2 - 0.3	0.3 - 0.4	0.4 - 0.5	0.5 - 0.6	0.6 - 0.7
slope 1:100		p9316/2	p9305/1	p9305/5	p9305/11	p9305/17	p9301/15
		p9313/2	p9313/17	p9304/7	p9310/17	p9302/17	p9303/15
slope 1:250		ss011/2	ss221/2	ss211/6	ss211/12	ss015/16	
	ss418/2	ss421/2	ss323/2	ss111/1	ss321/7	ss426/19	

The numbers in Table 4.2 refer to the test run and the location of the wave gauge, at which the data of that particular run were obtained.

Secondly, a set of tests is selected to validate the proposed local wave height distribution model. These validation data are presented in Table 4.3. Since the wave height distributions of wave fields on shallow foreshores with a high relative wave height are most interesting a non-homogeneous selection of tests for the validation data is made. Therefore Table 4.3 shows an excess of test runs with a high relative wave height.

Table 4.3: Validation data ($\overline{H_{1/3} / d} = 0.434$).

local $H_{1/3}/d$	0 - 0.1	0.1 - 0.2	0.2 - 0.3	0.3 - 0.4	0.4 - 0.5	0.5 - 0.6	0.6 - 0.7
slope 1:100		p9308/3	p9310/7	p9311/17	p9307/13	p9309/17	p9304/15
		p9312/3	p9314/15	p9315/15	p9306/11	p9305/17	p9302/15
slope 1:250			ss418/5	ss318/5	ss223/9	ss421/15	ss013/17
				ss419/5	ss320/6	ss428/14	ss017/15
					ss420/9	ss226/14	
						ss328/15	
						ss329/18	

The fit procedure described in Section 3.3.3 has been applied to the selected calibration data. The results are presented in the following chapter.

5 Parameterisation

The Composed Weibull distribution, with the assumptions about the values of the exponents (k_1=2 and k_2=3.5) and the continuity condition (3.3), still contains two independent parameters. When H_2 is expressed in terms of H_1, using the continuity condition (3.3), these two independent parameters are H_1 and H_{tr}. In order to relate the Composed Weibull distribution to the output of wave energy propagation models parameterisations are developed for H_1 and H_{tr}, as a function of the degree of saturation. Therefore H_1 and H_{tr} are nondimensionalized, by dividing them by the square root of the water surface elevation variance.

5.1 Scale factor H_1

The fit procedure is applied to the tests of the calibration data. The results of the parameter estimation for the scale factor H_1 are presented in Figure 5.1.

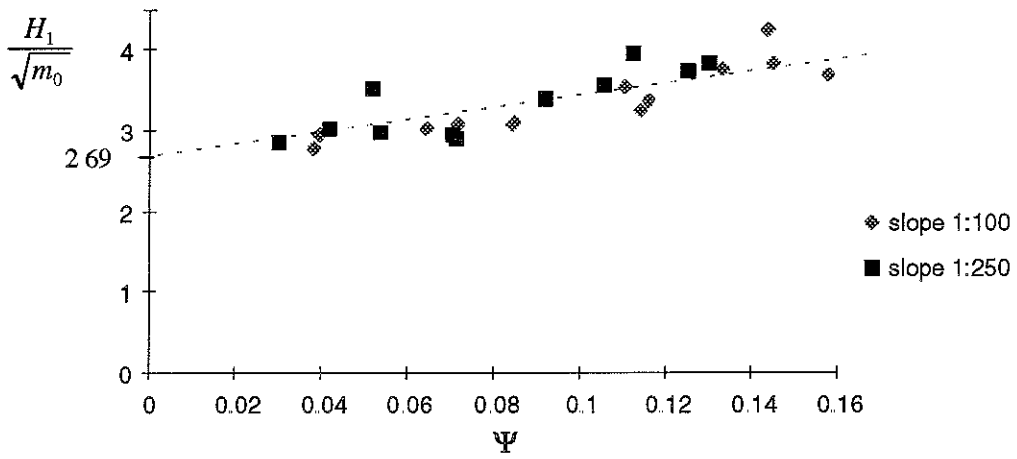

Figure 5.1: Estimated values of the nondimensional scale factor H_1 versus the degree of saturation. Calibration data.

Before a least squares optimisation method is unleashed to obtain an empirical forecasting function, the nondimensional H_1 is evaluated for low degrees of saturation. A low degree of saturation indicates relatively deep water. In deep water ($\Psi \rightarrow 0$) the wave heights obey the Rayleigh distribution. For $\Psi = 0$:

$$Q_H(H) = \exp\left[-2\left(\frac{H}{H_{1/3}}\right)^2\right] = \exp\left[-\left(\frac{H}{H_1}\right)^2\right] \tag{5.1}$$

Thus

$$H_1 = \frac{1}{\sqrt{2}} H_{1/3} \tag{5.2}$$

which, using (2.3), yields $H_1 = 2.69\sqrt{m_0}$

One can assume that the trend, shown in Figure 5.1, represents a linear relation between the nondimensional H_1 and the degree of saturation. Therefore the following forecasting function is proposed:

$$\frac{H_1}{\sqrt{m_0}} \approx 2.69 + \alpha_{H1}\Psi \tag{5.3}$$

The coefficient α_{H1} has been determined by fitting (5.3) to the data presented in Figure 5.1, using a least squares method. The dotted line represents (5.3) with $\alpha_{H1} = 8.1$.

5.2 Transitional wave height H_{tr}

In this section forecasting functions for the transitional wave height are proposed. First a purely empirical relation is obtained. Then more physically based forecasting functions are evaluated.

5.2.1 Empirical forecasting function H_{tr}

The results of the parameter estimation, as far as the transitional wave height H_{tr} is concerned, are presented in Figure 5.2.

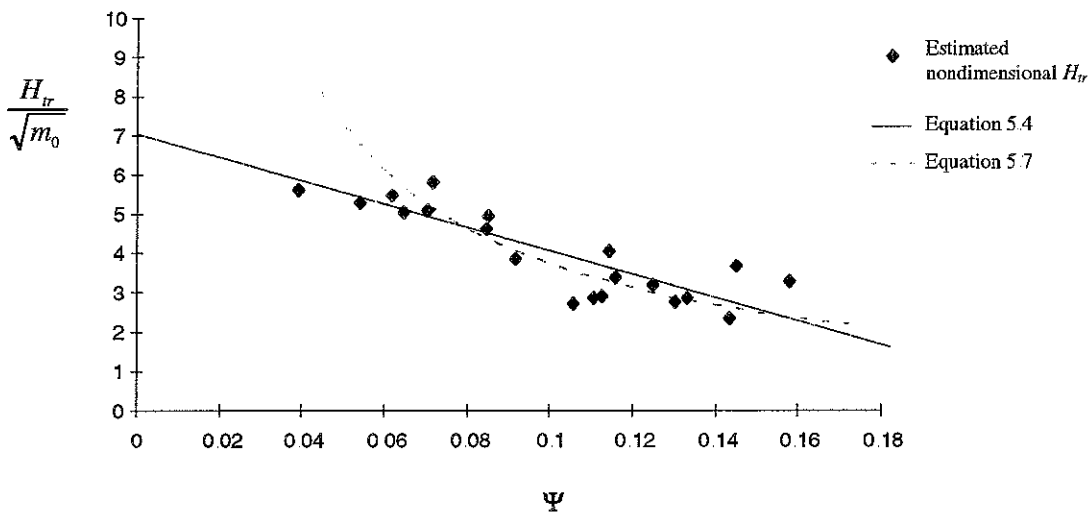

Figure 5.2: Estimated nondimensional transitional wave height versus the degree of saturation. Calibration data.

From Figure 5.2 an empirical forecasting function is obtained. Assuming a linear relation,

$$\frac{H_{tr}}{\sqrt{m_0}} \approx \alpha_{tr} - \beta_{tr}\Psi \tag{5.4}$$

in which α_{tr} and β_{tr} are constants to be determined empirically. Using a least squares optimisation method (5.4) is fitted to the data presented in Figure 5.2. The dotted line represents (5.4) with $\alpha_{tr} = 7.0$ and $\beta_{tr} = 31.3$.

5.2.2 Semi-empirical forecasting function H_{tr}

In the previous section a purely empirical relation is obtained to describe the nondimensional transitional wave height as a function of the degree of saturation. However, a forecasting function with some physical foundation is preferred.

The transitional wave height is the wave height at which the wave height distribution abruptly changes its shape. The change in shape is a result of depth-induced breaking of the waves exceeding the transitional wave height. Therefore the following hypothesis is posed:

$$H_{tr} \sim d \tag{5.5}$$

The transitional wave heights obtained in the parameter estimation, nondimensionalized with the water depth, have been plotted as a function of the degree of saturation in Figure 5.3.

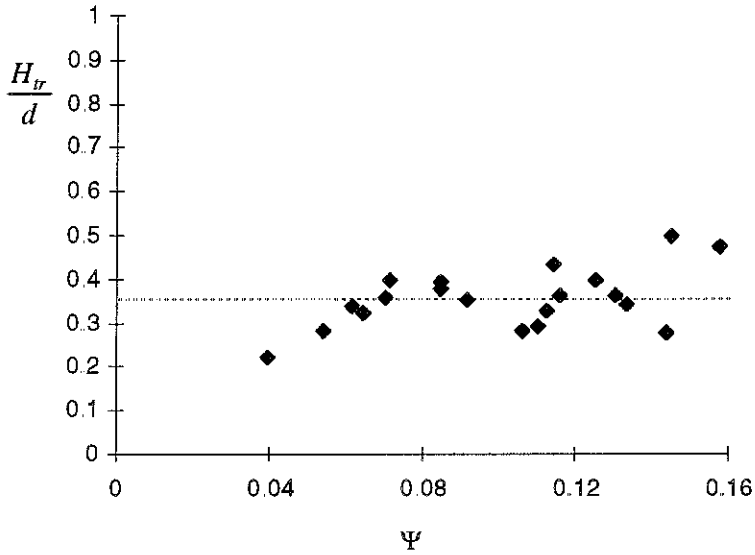

***Figure 5.3** Ratio of transitional wave height to water depth versus the degree of saturation. Calibration data.*

Figure 5.3 supports the hypothesis (5.5). Therefore, the transitional wave height can be related to the water depth via a coefficient, γ_{tr}:

$$H_{tr} = \gamma_{tr} d \tag{5.6}$$

In Figure 5.3 the dotted line represent a line with $H_{tr}/d = 0.36$. Expressed in terms of Ψ, (5.6) implies that

$$\frac{H_{tr}}{\sqrt{m_0}} = \gamma_{tr} \Psi^{-1} \tag{5.7}$$

This relation is plotted in Figure 5.2. In Figure 5.4 the nondimensional transitional wave height is plotted versus Ψ^{-1}. In this graph the dotted line represents equation (5.6) with $\gamma_{tr} = 0.36$. In this graph an overestimation of the nondimensional transitional wave height for the higher values of Ψ^{-1} is observed. The higher values of Ψ^{-1} represent relatively deep water. In relatively deep water the waves are mainly limited by the maximum wave steepness. Hence, (5.6) overestimates the transitional wave height for $\Psi^{-1} \gtrsim 16$ (i.e. $\Psi \lesssim 0.06$).

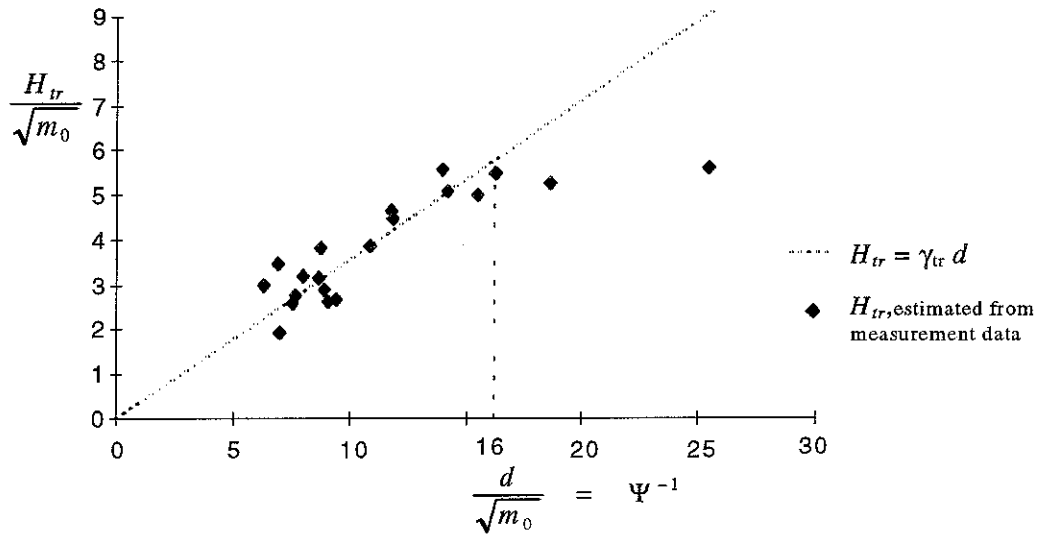

Figure 5.4: Nondimensional transitional wave height versus Ψ^{-1}. Calibration data.

High degrees of saturation (i.e. low values of Ψ^{-1}) are the most interesting. These high degrees of saturation represent relatively shallow water in which the wave height distribution strongly deviates from the Rayleigh distribution. The semi-empirical relation (5.6) yields a reasonably good prediction of the transitional wave height for high relative wave heights (i.e. low values of Ψ^{-1}).

5.2.3 Miche-like forecasting function H_{tr}

Miche (1944) defined a maximum wave height of a regular wave. In deep water the maximum wave height is determined by a maximum wave steepness. In shallow water depth-induced breaking dominates the wave deformation process, therefore in shallow water the maximum wave height is related to the water depth. When it is assumed that the transitional wave height is related to Miche's maximum wave height, the following relation could describe H_{tr}:

$$H_{tr} = \alpha_t\, 0.14\, L_{0,2} \tanh\left(\frac{2\pi d}{L_{0,2}}\right) \tag{5.8}$$

in which α_t denotes an empirical coefficient and $L_{0,2}$ is the local wavelength, defined by:

$$L_{0,2} = \frac{gT_{0,2}^2}{2\pi} \tanh\left(\frac{2\pi d}{L_{0,2}}\right) \tag{5.9}$$

$T_{0,2}$ is the average zero-crossing wave period for a stationary Gaussian process, derived by Rice (1944):

$$T_{0,2} = \left(\frac{m_0}{m_2}\right)^{\frac{1}{2}} \tag{5.10}$$

in which m_0 and m_2 are the local zero-th and second spectral moments. Equation 5.9 is to be solved by iteration or can be approximated by:

$$L_{0,2} = L_0\left(1-\exp\left[-\left(2\pi\frac{d}{L_0}\right)^{1.25}\right]\right)^{0.4} \qquad \varepsilon < 8\cdot10^{-3} \tag{5.11}$$

in which

$$L_0 = \frac{gT_{0,2}^2}{2\pi} \tag{5.12}$$

The empirical coefficient α_t in (5.8) is calibrated by comparing estimated and computed values of the nondimensional transitional wave height, using equation (5.8). A least squares optimisation method results in $\alpha_t \approx 0.52$. In Figure 5.5 the estimated nondimensional transitional wave heights are compared to the nondimensional transitional wave heights obtained with (5.8), for $\alpha_t = 0.52$. (Using this value of α_t, Equation 5.8 yields $\gamma_{tr} \equiv 0.28\pi\alpha_t \approx 0.46$ in very shallow water.)

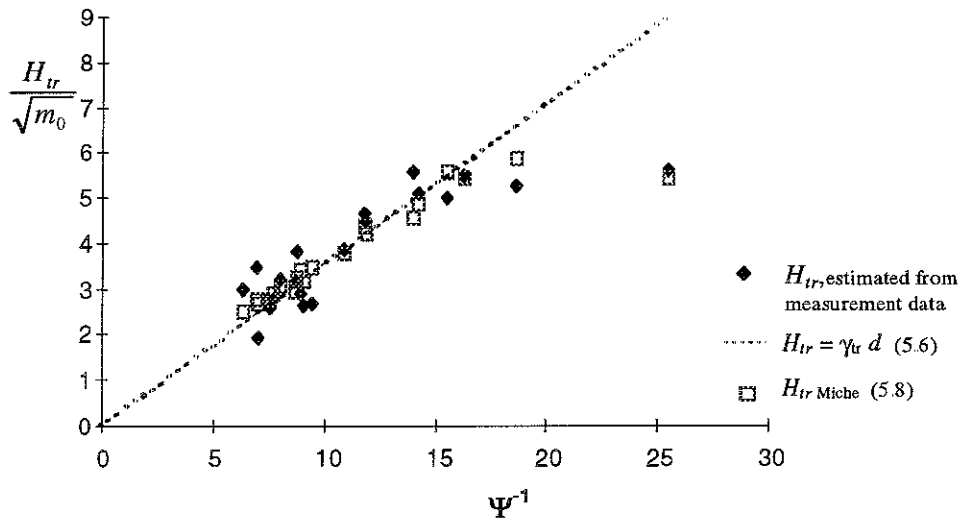

Figure 5.5: Comparison of computed and estimated transitional wave heights. Calibration data.

Figure 5.5 shows that a Miche-like forecasting function yields a better approximation of the estimated transitional wave heights than Equation 5.6, for low degrees of saturation (i.e. high values of Ψ^{-1}).

5.2.4 Discussion of forecasting functions for H_{tr}

In this section three different parameterisations of the transitional wave height are described. A forecasting function with some physical foundation is preferred, such as (5.6) and (5.8). Still the following drawbacks of these forecasting functions must be noted:

- The forecasting function based on a breaker criterion, depending on the water depth only, does not give a good prediction of the transitional wave height for low degrees of saturation.

- The second order spectral moment weights the energy at the higher frequencies more heavily than lower order spectral moments. Therefore m_2 more is sensitive to higher harmonics. This makes the Miche-like forecasting function (5.8) less robust.
- In extreme shallow water the assumption of a Gaussian water surface elevation is violated. Therefore the expression for the average zero-crossing period, as derived by Rice (1944), is not valid.

A quantitative evaluation of transitional wave height forecasting functions is presented in Chapter 6.

5.3 Concluding comment

Using the results of the parameterisation mentioned above, H_1 and H_{tr} are known for given water depth (d) and energy spectrum of the waves (m_0, m_2, etc.) and a fully predictive model is obtained without independent parameters (Once a choice has been made among the alternative transitional wave height forecasting functions). In Figure 5.6 a flowchart of the application of the Composed Weibull distribution model is presented.

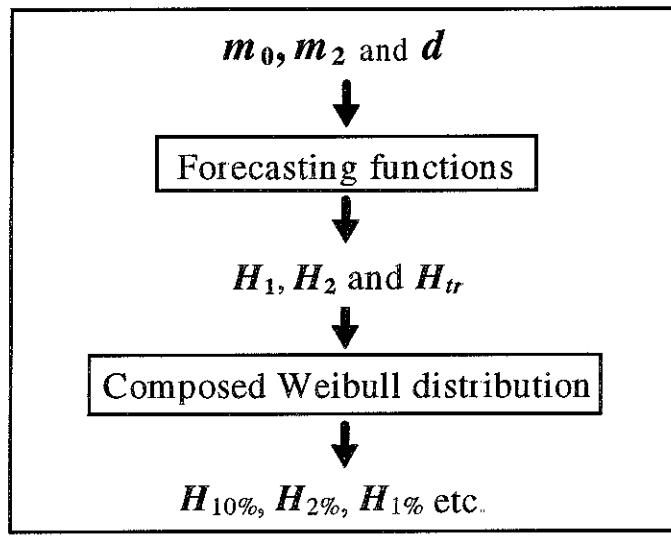

***Figure 5.6**: Flowchart of the application of the Composed Weibull distribution model.*

The Composed Weibull distribution model as described in Figure 5.6 is validated in the following chapter.

6 Validation

The validation is carried out by comparing the proposed distribution and the New Modified Glukhovskiy distribution for both used and new laboratory data. Used laboratory data refers to the calibration data. When calibration data is used for validation, some inbreeding is to be expected. However, still some valuable information about the behaviour of the Composed Weibull wave height distribution, compared to the Rayleigh distribution and the New Modified Glukhovskiy distribution, is obtained. In Section 6.2 a real validation is carried out with new data, called validation data (see Section 4.3). The validation with calibration data is described below.

6.1 Validation with calibration data

In this section the Composed Weibull distribution model is compared to existing wave height distribution models. The data used in this comparison are the calibration data. First, some measured wave height distributions and corresponding computed Composed Weibull distributions are presented, in order to illustrate the performance of this distribution.

6.1.1 Computed Composed Weibull wave height distributions

The following two graphs show two measured wave height distributions for different degrees of saturation. From the corresponding measured local spectral moments and water depth the parameters H_{tr} and H_1 have been determined, using (5.8) and (5.3). Hence, the Composed Weibull distribution is obtained.

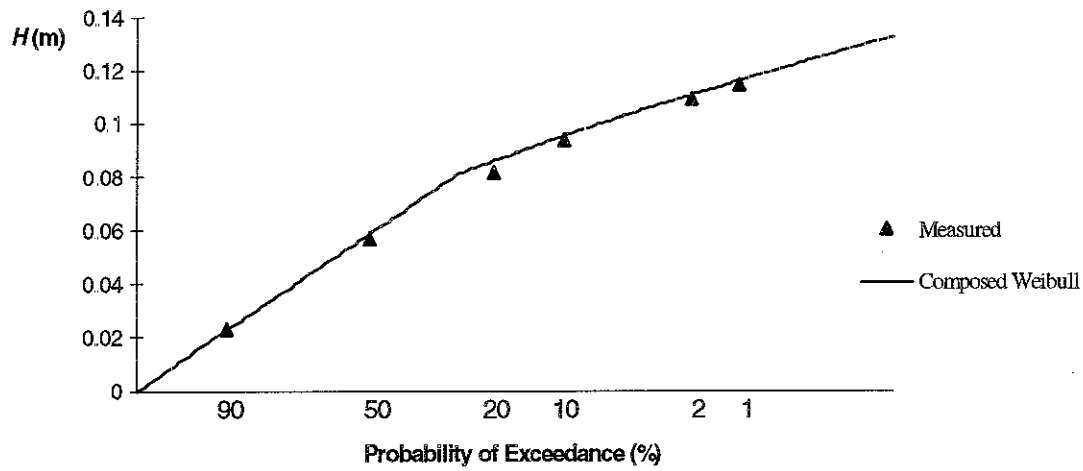

Figure 6.1: Computed Composed Weibull distribution (m_0=4.27e-4 m^2, d=0.225 m and Ψ=0.092). Calibration data.

Both Figure 6.1 and Figure 6.2 show a good approximation of the measured wave height distribution by the Composed Weibull distribution. An overall validation and a comparison of the Composed Weibull distribution model comparison to existing shallow water wave height distribution models is presented in the following sections.

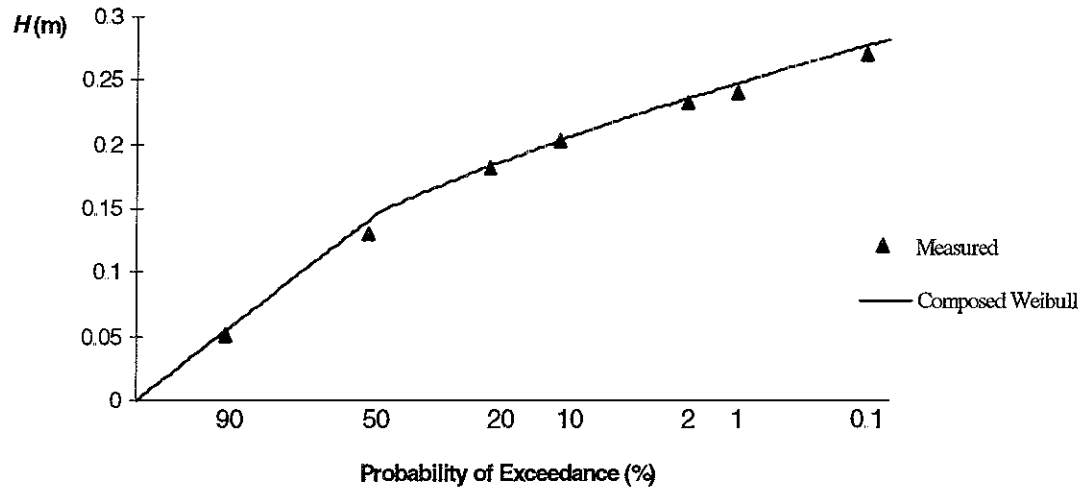

Figure 6.2: Computed Composed Weibull distribution (m_0=2.26e-3 m^2, d=0.41 m and Ψ=0.116) Calibration data

6.1.2 Comparison to existing wave height distribution models

In order to obtain a global view of the performance of the Composed Weibull distribution compared to the Rayleigh distribution and the New Modified Glukhovskiy distribution, computed characteristic nondimensional wave heights are presented below. In the following graphs measured characteristic wave heights are compared to computed characteristic wave heights. In all computations of characteristic wave heights presented below, the measured local m_0 and d are used as input for the Rayleigh distribution (2.1) and the New Modified Glukhovskiy distribution (2.10). The transitional wave height of the Composed Weibull distribution is computed with the Miche-like forecasting function (5.8). Therefore in the computation of characteristic wave heights with the Composed Weibull distribution the measured local second spectral moment m_2 is also used as input.

In Figure 6.3 a comparison of relative significant wave height for the three distributions is presented.

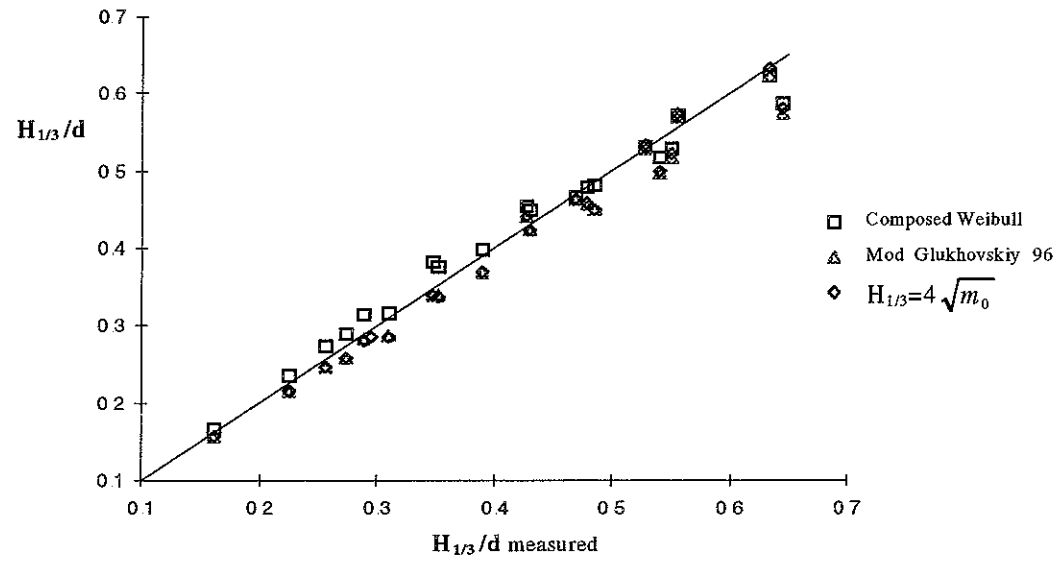

Figure 6.3: Computed and measured relative significant wave heights for Calibration data.

For the lower relative significant wave heights a slight overestimation of the significant wave height by the Composed Weibull distribution and a slight underestimation by the New Modified Glukhovskiy distribution is observed. In general, all distributions give a good approximation of the measured significant wave height.

The differences between the Composed Weibull distribution model and the New Modified Glukhovskiy distribution become more clear when the ratio of the wave height with a low probability of exceedance to the significant wave height is evaluated as a function of the degree of saturation. In Figure 6.4 the results for $H_{10\%}/H_{1/3}$ are presented.

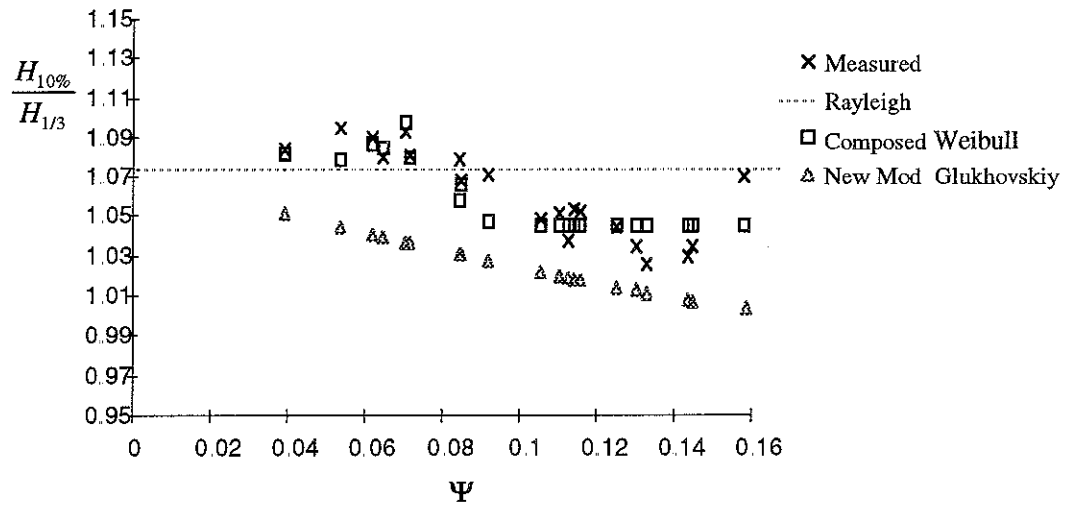

Figure 6.4: Computed and measured $H_{10\%}$ to $H_{1/3}$ ratio as function of the degree of saturation. Calibration data

In Figure 6.4 an underestimation of $H_{10\%}/H_{1/3}$ by the New Modified Glukhovskiy distribution is observed. This is caused by an underestimation of the wave heights with an exceedance probability of 1/10, as shown in Figure 6.5.

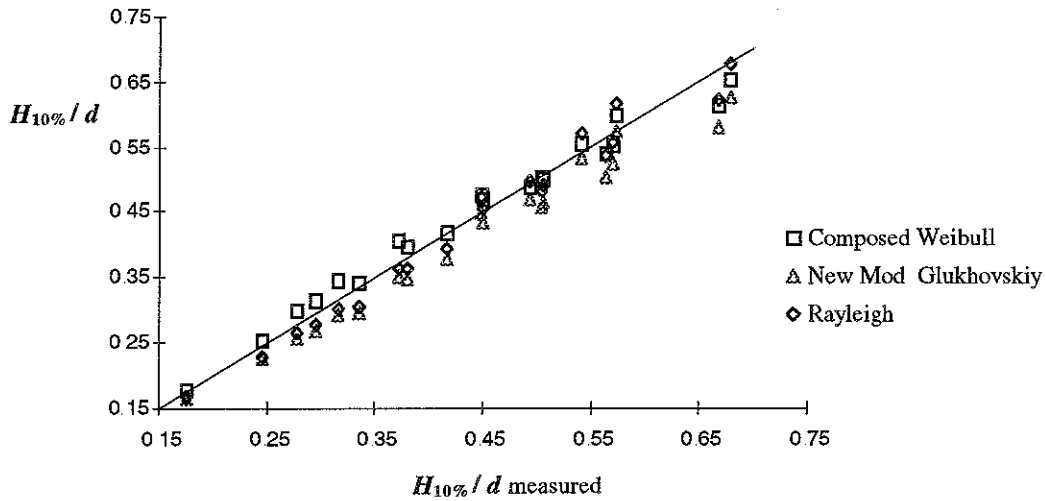

Figure 6.5: Computed and measured $H_{10\%}$ to water depth ratio. Calibration data

When extreme wave heights are concerned the Rayleigh distribution can no longer be applied. Both the Composed Weibull and the New Modified Glukhovskiy distribution yield an

approximation of the measured extreme wave heights far better than the Rayleigh distribution, as shown in Figure 6.6.

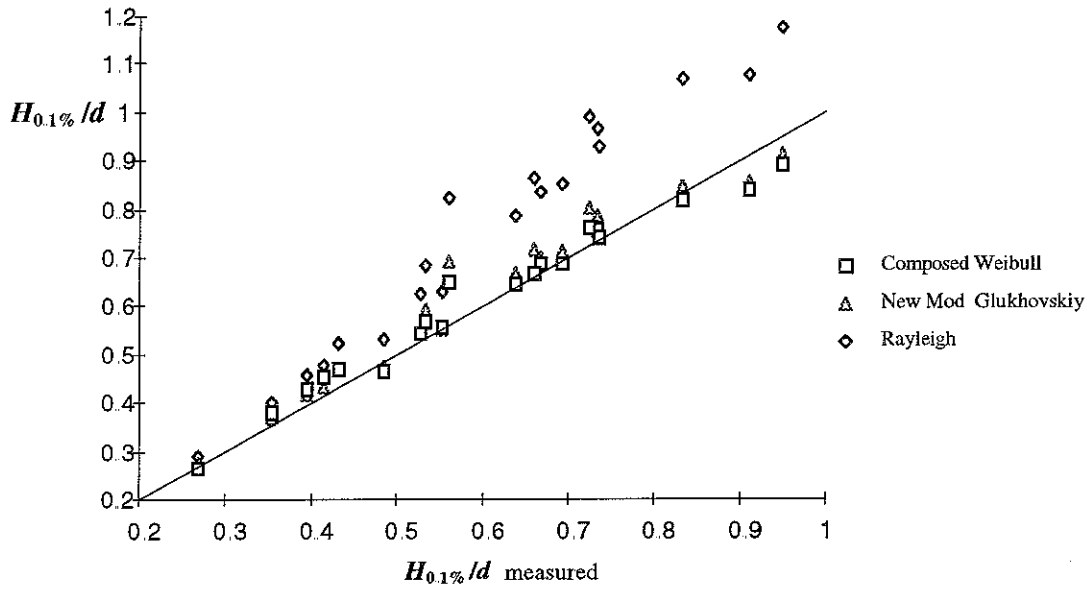

***Figure 6.6**: Computed and measured $H_{0.1\%}$ to water depth ratio. Calibration data.*

However, the Modified Glukhovskiy distribution overestimates the $H_{0.1\%}$ to $H_{1/3}$ ratio, as shown in Figure 6.7.

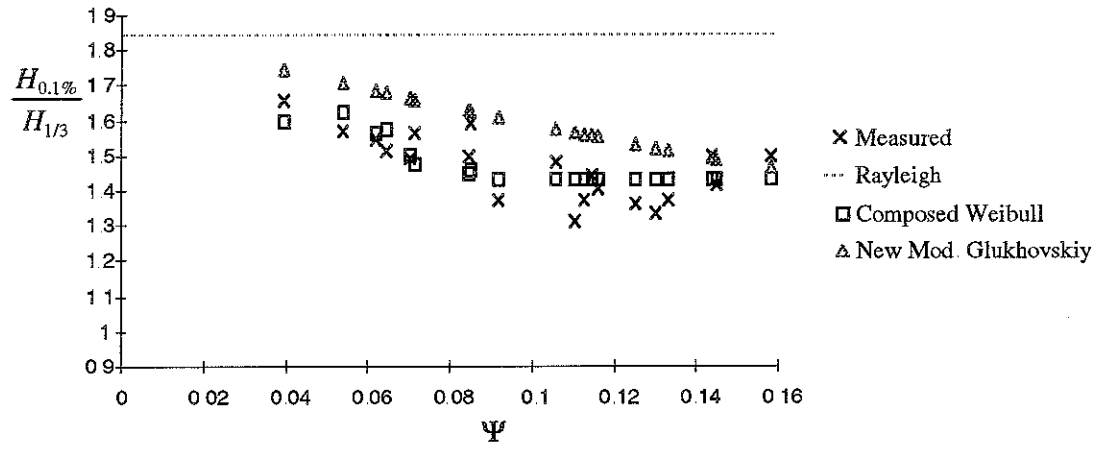

***Figure 6.7**: Computed and measured $H_{0.1\%}$ to $H_{1/3}$ ratio Calibration data.*

This overestimation by the New Modified Glukhovskiy distribution will increase for wave heights with a smaller probability of exceedance. This distribution cannot describe all wave heights in the wave height distribution on a shallow foreshore as well as the Composed Weibull distribution. This may be due to the fact that the New Modified Glukhovskiy distribution uses the same function both for the lower (nonbreaking) and the higher (breaking) waves, in contrast to the Composed Weibull distribution.

6.1.3 Root mean square error

An indicator of the overall approximation of the measured wave height distribution by the three local wave height distribution models is the normalised root mean square error ε_{rms}, defined as:

$$\varepsilon_{rms} = \sqrt{\frac{1}{i}\sum_{1}^{i}\left(\frac{H_{N,comp}}{H_{N\,meas}}-1\right)^2} \qquad (6.1)$$

in which i denotes the number of tests used to determine the root mean square error and H_N denotes a wave height with probability of exceedance equal to $1/N$. For each local wave height distribution model the root mean square error is determined for five values of N. In Section 5.2 three different transitional wave height forecasting functions for the Composed Weibull distribution model are described. A quantitative evaluation of these forecasting functions is obtained by computing the root mean square error of the Composed Weibull distribution model for different forecasting functions. The results are presented in Table 6.1.

***Table 6.1**: Root mean square error (calibration data).*

	$H_{50\%}$	$H_{10\%}$	$H_{2\%}$	$H_{1\%}$	$H_{0.1\%}$	
	ε_{rms}					$\overline{\varepsilon_{rms}}$
Rayleigh	0.179	0.049	0.103	0.138	0.247	**0.143**
Mod. Glukhovskiy (Klopman 1996)	0.122	0.078	0.064	0.057	0.078	**0.080**
Composed Weibull (Empirical H_{tr})	0.084	0.066	0.059	0.063	0.080	**0.070**
Composed Weibull (Miche-like H_{tr})	0.079	0.049	0.048	0.048	0.063	**0.057**
Composed Weibull ($H_{tr}=\gamma_{tr}\,d$)	0.079	0.059	0.058	0.212	0.209	**0.123**
Composed Weibull ($H_{tr}=\gamma_{tr}\,d\ \Psi>0.06$)	0.084	0.061	0.056	0.059	0.074	**0.067**

The overall root mean square error in Table 6.1 clearly shows that the modified Glukhovskiy distribution and the Composed Weibull distribution model achieve a far better approximation of the measured wave height distributions than the Rayleigh distribution. The overall root mean square errors of the Composed Weibull distribution model for different transitional wave height forecasting functions yield some interesting information.

The best approximation of the measured wave height distributions is achieved when the Miche-like transitional wave height forecasting function (5.8) is used in the Composed Weibull distribution model. However, as stated in Section 5.2.4, this forecasting function has the disadvantage of a third input parameter m_2. Therefore, a forecasting function like (5.6) is preferred. As stated in Section (5.2.4), the disadvantage of this forecasting function is that for low degrees of saturation (low values of $H_{1/3}/d$) the transitional wave height is strongly overestimated. Hence, a limitation to the validity of this forecasting function is introduced. Since mainly the high degrees of saturation are of interest, the root mean square error of the Composed Weibull distribution model is computed using only the tests obeying $\Psi > 0.06$. The results of this limitation are presented in the last row of Table 6.1. Limiting of the Composed Weibull distribution model to wave fields obeying $\Psi > 0.06$ yields a more satisfying root mean square error.

However, no definite conclusions can be drawn, since this validation is based on the calibration data. A validation based on new data is presented in the following section.

6.2 Validation with new data

In this section the New Modified Glukhovskiy distribution and the Composed Weibull distribution model are compared using new data. New data refers to data not used in the parameterisation. First however, some graphs demonstrate the ability of the Composed Weibull distribution to approximate measured shallow foreshore wave height distributions, which have not be used in the calibration.

6.2.1 Computed Composed Weibull wave height distributions

The following graphs show measured wave height distributions for different degrees of saturation. From the corresponding measured local spectral moments and water depth the parameters H_{tr} and H_1 have been determined, using (5.7) and (5.3). The graphs support the validity of the model in a qualitative sense.

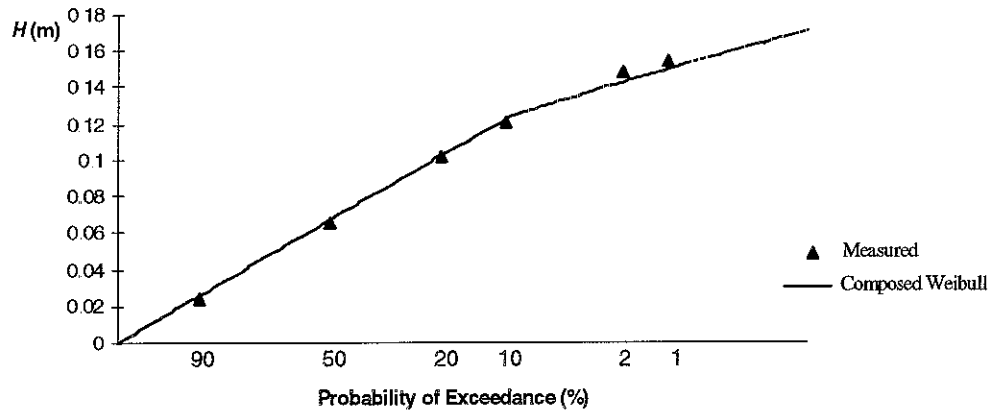

Figure 6.8: Computed Composed Weibull distribution (m_0=6.16e-4 m^2, d=0.33 m and Ψ=0.075). Validation data.

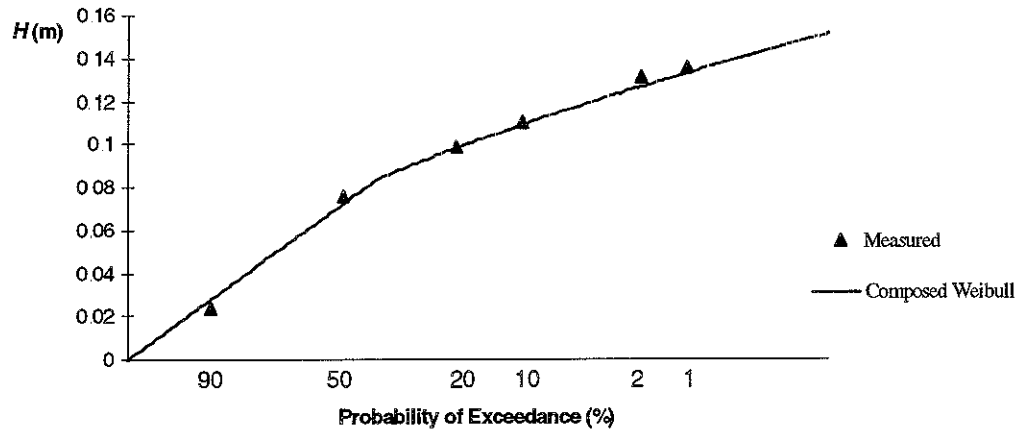

Figure 6.9: Computed Composed Weibull distribution (m_0=5.85e-4 m^2, d=0.21 m and Ψ=0.115). Validation data

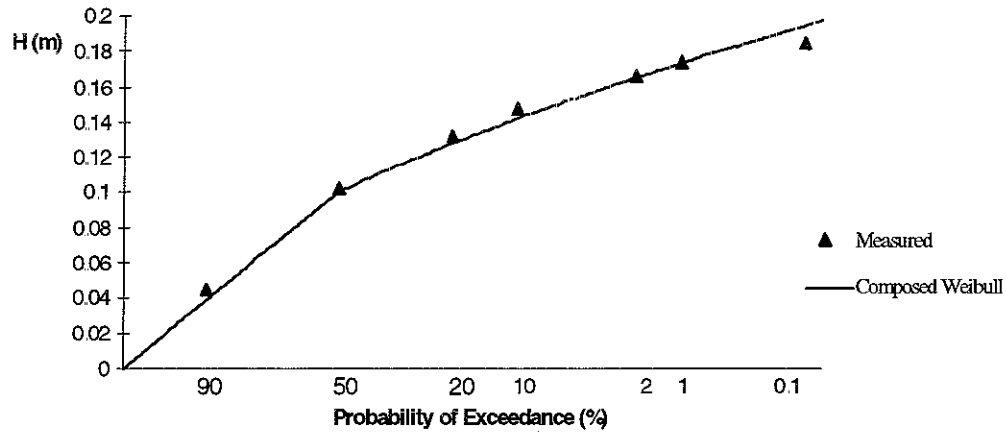

Figure 6.10: Computed Composed Weibull distribution (m_0=1 10e-3 m^2, d=0.26 m and Ψ=0 128). Validation data

An overall validation and a comparison of the Composed Weibull distribution model to existing shallow water wave height distribution models are presented in the following sections.

6.2.2 Comparison to existing wave height distribution models

As in Section 6.2, model predictions of $H_{10\%}/H_{1/3}$ and $H_{0.1\%}/H_{1/3}$ are evaluated as a function of the degree of saturation. In Figure 6.11 and 6.12 the results for wave heights with an exceedance probability of 1/10 are shown.

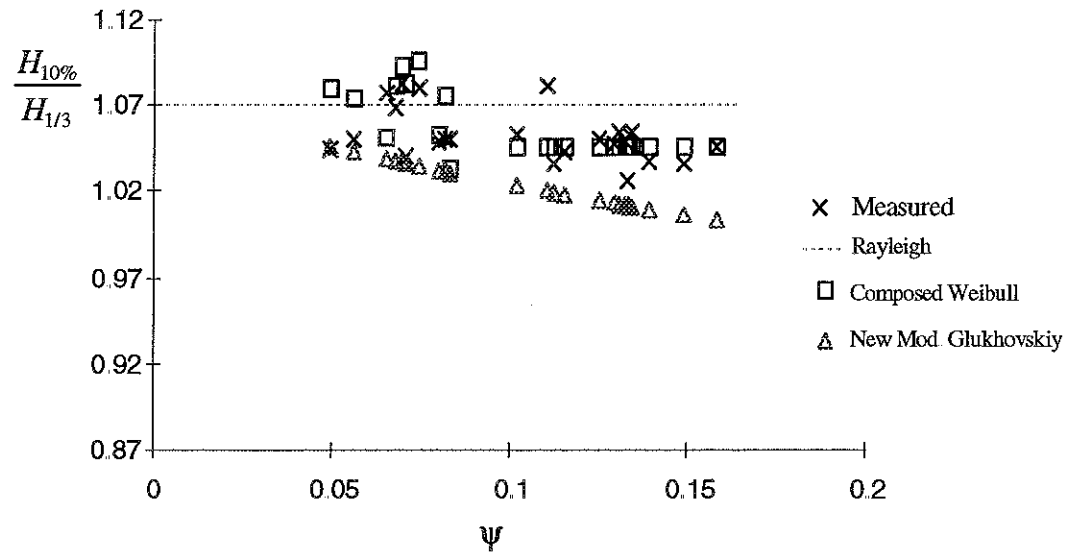

Figure 6.11: Computed and measured $H_{10\%}$ to $H_{1/3}$ ratio as function of the degree of saturation. Validation data

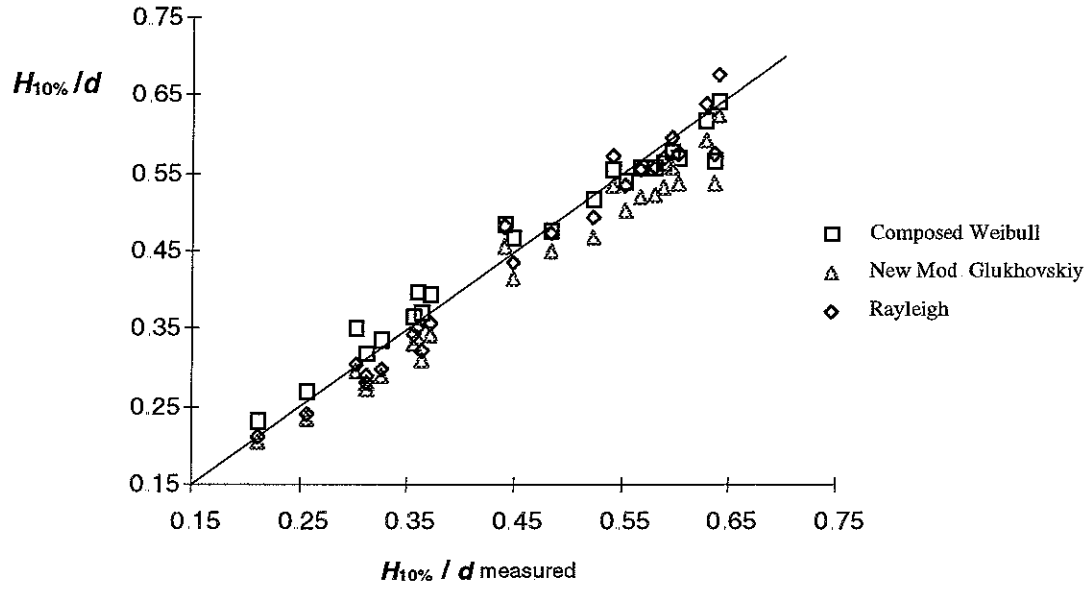

Figure 6.12: Computed and measured $H_{10\%}$ to water depth ratio. Validation data.

Clearly the same trend as in Section 6.1 is observed. The New Modified Glukhovskiy distribution underestimates $H_{10\%}$, which results in an underestimation of the $H_{10\%}/H_{1/3}$ ratio. In the Figures 6.13 and 6.14 the results for $H_{0.1\%}$ are shown.

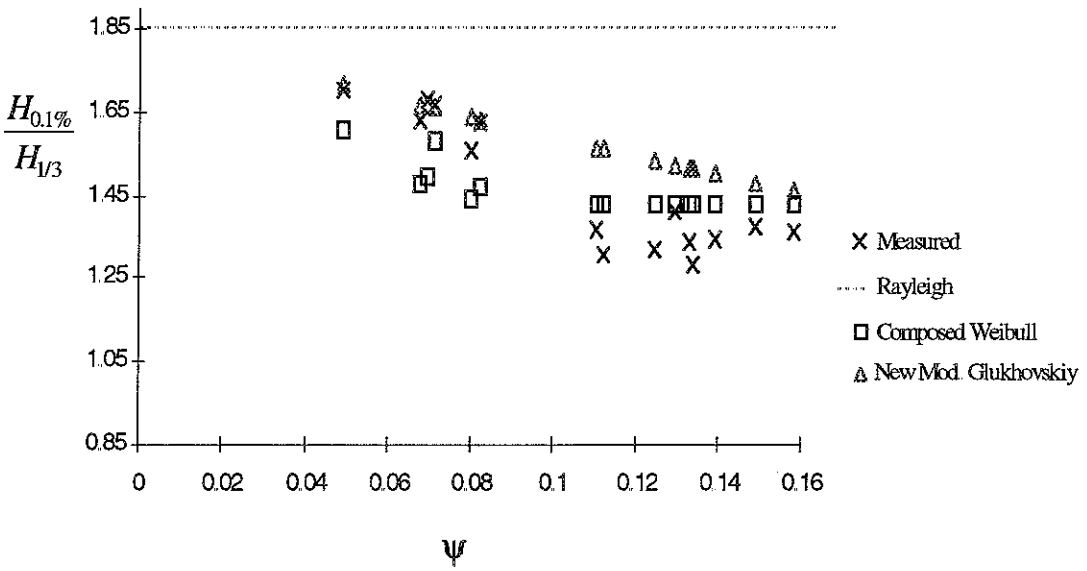

Figure 6.13: Computed and measured $H_{0.1\%}$ to $H_{1/3}$ ratio as function of the degree of saturation. Validation data.

Again, as in Section 6.2, the Composed Weibull distribution model gives a slightly better approximation than the New Modified Glukhovskiy distribution.

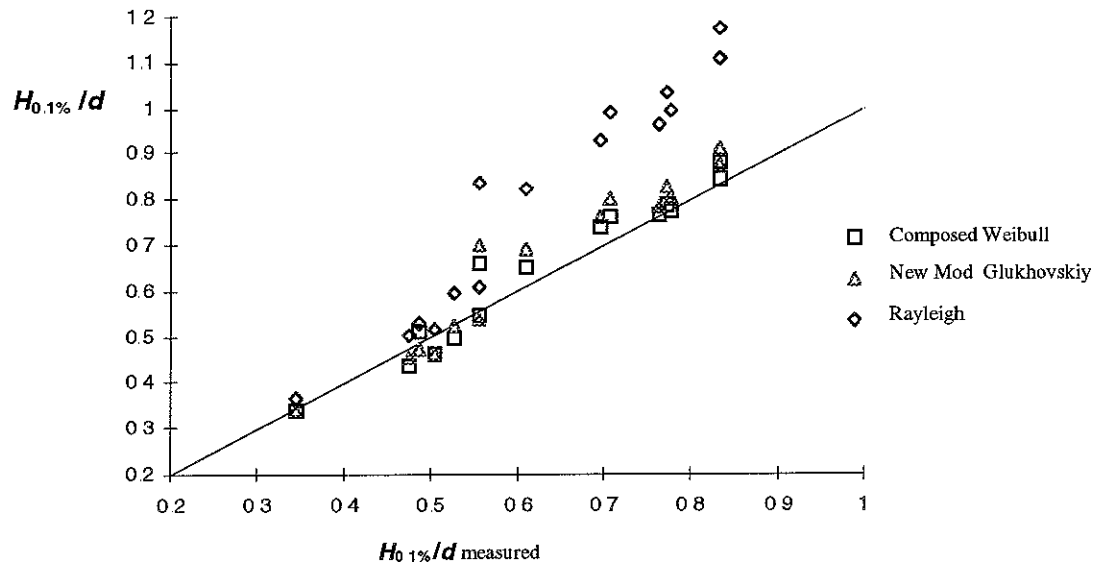

Figure 6.14: Computed and measured $H_{10\%}$ to water depth ratio. Validation data

6.2.3 Root mean square error

A more global comparison between the Rayleigh distribution, the New Modified Glukhovskiy and the Composed Weibull distribution is carried out by determining the normalised root mean square error, using Equation 6.1. The results are presented below.

Table 6.2: Relative root mean square error (validation data)

	$H_{50\%}$	$H_{10\%}$	$H_{2\%}$	$H_{1\%}$	$H_{0.1\%}$	
	ε_{rms}					$\overline{\varepsilon_{rms}}$
Rayleigh	0.196	0.057	0.119	0.146	0.285	**0.161**
New Modified Glukhovskiy	0.138	0.087	0.089	0.091	0.097	**0.100**
Composed Weibull (Empirical H_{tr})	0.072	0.071	0.067	0.076	0.081	**0.073**
Composed Weibull (Miche-like H_{tr})	0.063	0.061	0.053	0.055	0.070	**0.061**
Composed Weibull ($H_{tr}=\gamma_{tr}\, d$)	0.073	0.072	0.059	0.125	0.069	**0.080**
Composed Weibull ($H_{tr}=\gamma_{tr}d$, Ψ>0.06)	0.075	0.072	0.061	0.065	0.063	**0.067**

The Composed Weibull distribution gives the best approximation of the measured wave height distributions. The reduction in root mean square error is about 60% compared to the Rayleigh distribution and about 30% compared to the New Modified Glukhovskiy distribution.

7 New constraint

In the previous chapters a local wave height distribution model has been obtained. This model is based on the Composed Weibull distribution. By assuming the shape of both distributions constant (k_1=2 and k_2=3.5) and using the continuity condition (3.3) as a constraint, only two parameters have to be predicted with forecasting functions. The Composed Weibull distribution model yields good approximations of measured wave height distributions, using the forecasting functions obtained in Chapter 5.

After finishing the validation of the Composed Weibull distribution model presented in the preceding chapters, a possible further simplification in the model has been investigated. The simplification is achieved by introducing a new constraint, based on physical arguments.

7.1 Root mean square wave height

If the total energy [J/m^2] of a wave field is given by:

$$E = \tfrac{1}{8}\rho g H_{rms}^2 \tag{7.1}$$

there is a relation between H_{rms} and $\sqrt{m_0}$ indifferent of the probability density function $f(H)$:

$$H_{rms} = \sqrt{8\, m_0} \tag{7.2}$$

Such a relation implies that H_{rms} is know a priori for given m_0. Here, relation (7.2) is investigated for shallow foreshores. Therefore measured values of $H_{rms}/\sqrt{m_0}$ have to be plotted versus the measured degree of saturation Ψ. However, the available data do not contain values of the measured root mean square wave heights. Hence, root mean square wave heights are obtained from wave height distributions fitted to the measured wave height distributions of the calibration data, using:

$$H_{rms} = \sqrt{\int_0^{H_{tr}} H^2\, f_1(H)dH + \int_{H_{tr}}^{\infty} H^2\, f_2(H)dH} \tag{7.3}$$

H_2 is determined by the continuity condition (3.4):

$$H_2 = H_{tr}\left(\frac{H_{tr}}{H_1}\right)^{-\frac{k_1}{k_2}} \tag{7.4}$$

and H_{tr} and H_1 are obtained by visual estimation. In Figure 7.1 these nondimensional root mean square wave heights are plotted versus the degree of saturation.

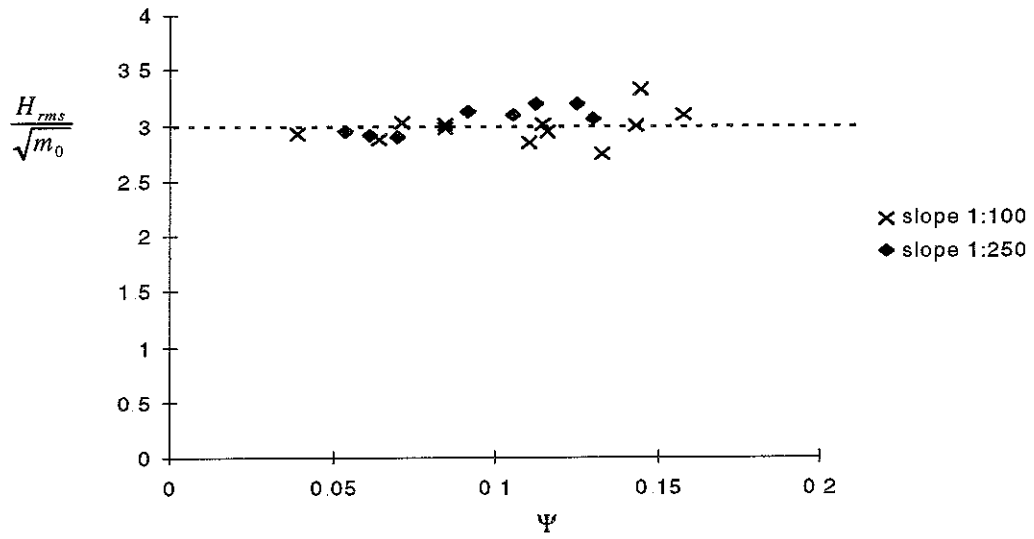

Figure 7.1 *Nondimensional H_{rms} versus the degree of saturation, calibration data.*

In Figure 7.1 a constant nondimensional H_{rms} is observed. However, instead of (7.2) one can observe in Figure 7.1 that

$$\frac{H_{rms}}{\sqrt{m_0}} \approx 3 \tag{7.5}$$

Figure 7.1 also shows that the nondimensional H_{rms} becomes smaller than 3 for low degrees of saturation. For real sea waves, with a broad banded frequency spectrum, the root mean square wave height in deep water is

$$H_{rms} \approx 0.95 \; 2\sqrt{2\, m_0} \approx 2.69\sqrt{m_0} \tag{7.6}$$

So one could try to obtain a function

$$\frac{H_{rms}}{\sqrt{m_0}} = f(\Psi) \tag{7.7}$$

which decreases for low degrees of saturation, with $f(0) \approx 2.69$. However, in the present study Equation 7.5 is used as a constraint.

7.2 New constraint

The Composed Weibull distribution has five parameters. With the assumptions about the values of its exponents and the continuity condition (3.3) only two independent parameters remain. In Section 5.2 a physically based forecasting function for H_{tr} has been obtained. In Section 7.1 the relation between H_{rms} and $\sqrt{m_0}$ is described. Using the relation (7.5) as a constraint and a forecasting function like (5.6), a fully predictive, physically based wave height distribution model is obtained, as shown below.

First, H_{rms} is expressed in terms of the parameters of the Composed Weibull distribution. Using the transformation and the gamma functions described in Appendix A, Equation 7.3 yields:

$$H_{rms} = \sqrt{H_1^2 \gamma\left[\frac{2}{k_1}+1, \left(\frac{H_{tr}}{H_1}\right)^{k_1}\right] + H_2^2 \Gamma\left[\frac{2}{k_2}+1, \left(\frac{H_{tr}}{H_2}\right)^{k_2}\right]} \quad (7.8)$$

or, with $k_1 = 2$ and $k_2 = 3.5$

$$H_{rms} = \sqrt{H_1^2 \gamma\left[2, \left(\frac{H_{tr}}{H_1}\right)^{2}\right] + H_2^2 \Gamma\left[\frac{11}{7}, \left(\frac{H_{tr}}{H_2}\right)^{3.5}\right]} \quad (7.9)$$

Now all wave heights are nondimensionalized by dividing them by H_{rms}:

$$\tilde{H}_x = \frac{H_x}{H_{rms}} \quad (7.10)$$

in which H_x denotes a characteristic wave height, $H_{1/3}$, $H_{1\%}$ etc. Normalizing all wave heights in (7.9) yields:

$$\tilde{H}_{rms} = 1 = \sqrt{\tilde{H}_1^2 \gamma\left[2, \left(\frac{\tilde{H}_{tr}}{\tilde{H}_1}\right)^{2}\right] + \tilde{H}_2^2 \Gamma\left[\frac{11}{7}, \left(\frac{\tilde{H}_{tr}}{\tilde{H}_2}\right)^{3.5}\right]} \quad (7.11)$$

Equation 7.11 together with the continuity condition (7.4) form a set of two (implicit) algebraic equations from which $\tilde{H}_1$ and $\tilde{H}_2$ can be calculated for each given $\tilde{H}_{tr}$. Once $\tilde{H}_1$ and $\tilde{H}_2$ have been determined all other desired normalized wave height values ($\tilde{H}_{1\%}$, $\tilde{H}_{1\%}$ etc.) can be calculated for each given $\tilde{H}_{tr}$. The results are show in Figure 7.2

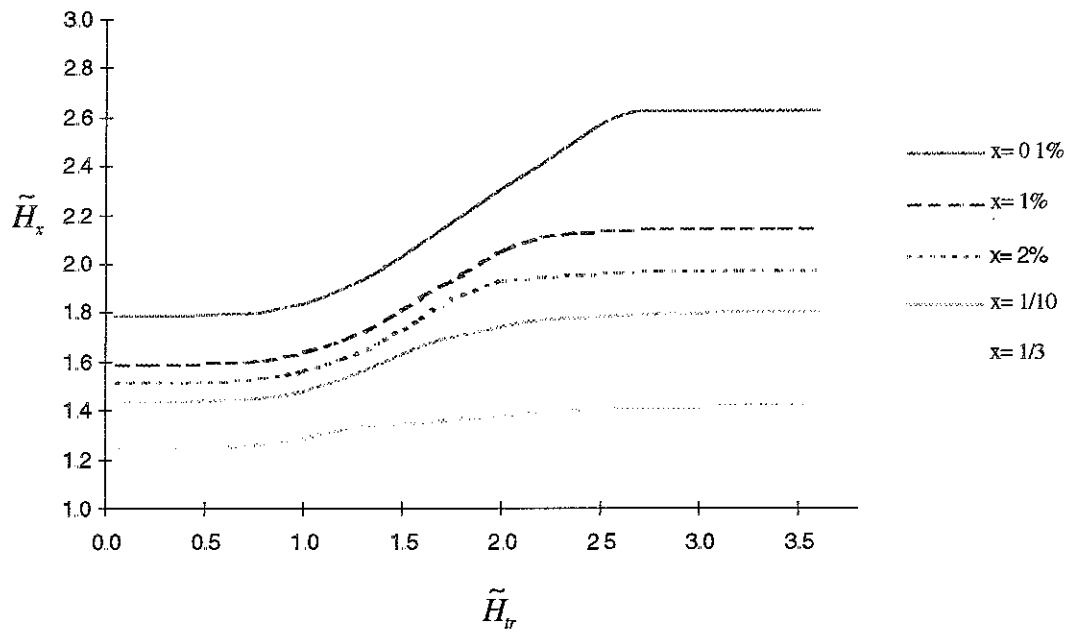

Figure 7.2: Characteristic nondimensional wave heights $\tilde{H}_x$ versus $\tilde{H}_{tr}$

In Table 7.1 the relations, as shown in Figure 7.3, are presented in tabular form. A more extensive table is presented in Appendix C.

Table 7.1: Characteristic nondimensional wave heights $\tilde{H}_x$ as function of $\tilde{H}_{tr}$

$\tilde{H}_{tr}$	$\tilde{H}_1$	$\tilde{H}_2$	$\tilde{H}_{1/3}$	$\tilde{H}_{1/10}$	$\tilde{H}_{2\%}$	$\tilde{H}_{1\%}$	$\tilde{H}_{0.1\%}$
0.05	9.949	1.029	1.249	1.438	1.520	1.592	1.788
0.2	3.518	1.029	1.249	1.438	1.520	1.592	1.788
0.4	2.092	1.030	1.250	1.438	1.520	1.593	1.789
0.6	1.549	1.032	1.252	1.441	1.523	1.596	1.792
0.8	1.265	1.040	1.262	1.452	1.535	1.608	1.806
1.0	1.106	1.059	1.285	1.479	1.564	1.638	1.840
1.2	1.021	1.094	1.321	1.528	1.616	1.693	1.901
1.4	0.983	1.144	1.338	1.597	1.689	1.769	1.987
1.6	0.970	1.202	1.350	1.669	1.775	1.860	2.088
1.8	0.971	1.265	1.364	1.714	1.868	1.957	2.197
2.0	0.977	1.328	1.379	1.744	1.933	2.055	2.307
2.2	0.985	1.390	1.392	1.766	1.947	2.113	2.414
2.4	0.991	1.448	1.402	1.781	1.960	2.126	2.515
2.6	0.995	1.502	1.409	1.791	1.969	2.136	2.609
2.8	0.998	1.553	1.413	1.796	1.974	2.141	2.623
3.0	0.999	1.601	1.414	1.798	1.976	2.144	2.626
3.2	1.000	1.646	1.415	1.799	1.977	2.145	2.627
3.4	1.000	1.689	1.416	1.800	1.978	2.146	2.628

To use the preceding results, for given d and $\sqrt{m_0}$, one still needs to determine H_{tr} and H_{rms}. A few alternative forecasting functions for H_{tr} are described in Chapter 5. Here we choose the simplest, physically based forecasting function $H_{tr} = \gamma_{tr}\, d$, with γ_{tr}=0.36. (In application, a Miche-like forecasting function could be used as well). The root mean square wave height is obtained by using $H_{rms} = 3\sqrt{m_0}$, as described in Section 7.1.

Now a fully predictive, physically based wave height distribution model has been obtained. The validity of the model is investigated in the following section.

7.3 Validation

Again, as in Section 6.3 the normalised root mean square error is used as an indicator of the overall approximation of measured wave height distributions (validation data only) by the Rayleigh, New Modified Glukhovskiy and Composed Weibull distribution (using $k_1 = 2$, $k_2 = 3.5$, $H_{rms} = 3\sqrt{m_0}$ and $H_{tr} = 0.36\,d$).

The root mean square errors of the Rayleigh distribution and the Modified Glukhovskiy distribution, as shown in Table 6.2, are again presented in Table 7.2. Also, the two smallest overall root mean square errors of the Composed Weibull distribution without the new constraint from Table 6.2, are shown in Table 7.2.

Table 7.2 Root mean square error (validation data)

	$H_{50\%}$	$H_{10\%}$	$H_{2\%}$	$H_{1\%}$	$H_{0.1\%}$	
	ε_{rms}					$\overline{\varepsilon_{rms}}$
Rayleigh	0.196	0.057	0.119	0.146	0.285	**0.161**
New Mod. Glukhovskiy	0.138	0.087	0.089	0.091	0.097	**0.100**
Composed Weibull						
Empirical H_1 and Miche-like H_{tr}	0.063	0.061	0.053	0.055	0.070	**0.061**
Empirical H_1 and $H_{tr} = \gamma_{tr} d$ $\Psi > 0.06$	0.075	0.072	0.061	0.065	0.063	**0.067**
Composed Weibull (with new constraint)						
$H_{rms} = 3\,(m_0)^{1/2}$ and $H_{tr} = \gamma_{tr} d$	0.056	0.049	0.056	0.061	0.072	**0.059**

Table 7.3 shows that the assumption of a constant nondimensional H_{rms} yields a Composed Weibull distribution model which achieves an approximation of measured wave height distributions just as good as the Composed Weibull distribution without the new constraint However, the advantage of the Composed Weibull distribution with the new constraint is that it fully depends on one simple and physically based parameter $\tilde{H}_{tr}$

In Table 7.2 the root mean square error of the Composed Weibull distribution with one independent parameter has been computed with $\tilde{H}_{tr}$ as described in Section 7.2. This means that forecasting function (5.6) has been used to calculate the transitional wave height. It must be noted that when using a Miche-like or empirical forecasting function for the transitional wave height an even better approximation of measured wave height distributions might have been achieved.

7.4 Recipe and example

The validation in Section 7.2 has shown that the Composed Weibull distribution with simple, physically based parameterisations can be used as a predictive model. Here a recipe for the application of the Composed Weibull distribution model is presented:

1. Given $\sqrt{m_0}$ and d, calculate $\tilde{H}_{tr} = 0.12\dfrac{d}{\sqrt{m_0}}$.

2. Read the corresponding value of the desired normalised wave height $\tilde{H}_x$ in Table 7.1 or Table C.1.

3. Calculate $H_x = 3\sqrt{m_0}\tilde{H}_x$

In the following section measurements are used to illustrate this recipe

7.4.1 Example

The following wave height distribution was measured in a wave flume (test p9305/17). It is presented on Rayleigh scale in Figure 7.3.

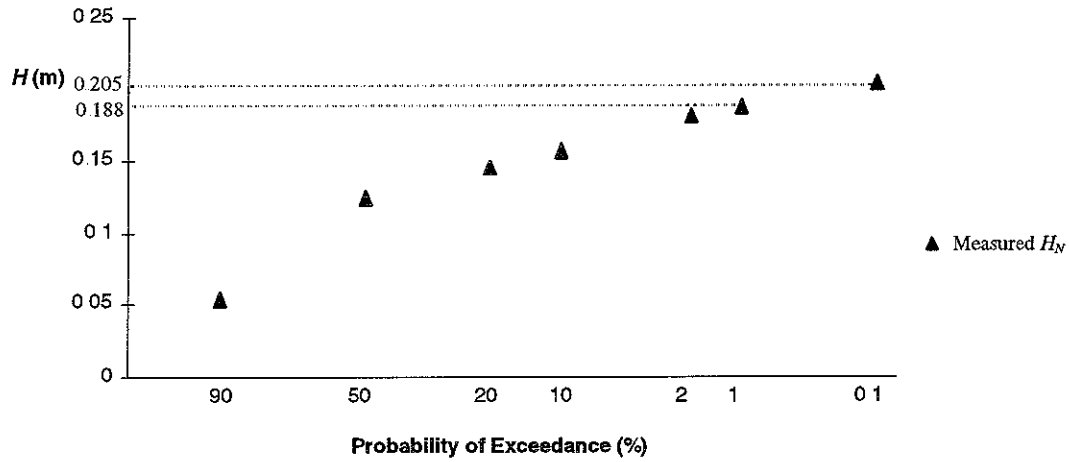

Figure 7.3 Measured wave heights with a certain probability of exceedance, validation data

The wave heights shown in Figure 7.3 were measured at water depth d = 0.29 m. At that depth the measured water surface elevation variance m_0 = 1.49e-3 m^2 (Ψ = 0.133) and the measured $H_{1/3}$ = 0.153 m.

$H_{1\%}$ is determined as follows:

1. $\tilde{H}_{tr} = 0.12\frac{d}{\sqrt{m_0}} = 0.902$.

2. Table C.1 (appendix C) yields $\tilde{H}_{1\%} \approx 1.62$.

3. $H_{1\%} = 3\sqrt{m_0}\tilde{H}_{1\%} = 0.188$ m. (Measured $H_{1\%}$ = 0.188 m.)

To calculate $H_{0.1\%}$ steps 2 and 3 are repeated:

2. Table (C.1 Appendix C) yields $\tilde{H}_{0.1\%} \approx 1.82$.

3. $H_{0.1\%} = 3\sqrt{m_0}\,\tilde{H}_{0.1\%} = 0.211$ m (Measured $H_{0.1\%}$ = 0.205 m.)

To calculate the significant wave height:

2. Table (C.1 Appendix C) yields $\tilde{H}_{1/3} \approx 1.27$.

3. $H_{1/3} = 3\sqrt{m_0}\,\tilde{H}_{1/3} = 0.147$ m. (Measured $H_{1/3}$ = 0.153 m.)

8 Conclusions and recommendations

The evolution of wave energy is well described by energy propagation models. These models can predict the water surface elevation variance at any location seaward of a sea-defence work. In deep water the wave height distribution is determined by the water surface elevation variance, since the wave heights obey the Rayleigh distribution. This is not the case in shallow water. Klopman (1996) empirically relates the Modified Glukhovskiy distribution to the local water depth and local water surface elevation. Hence, Klopman (1996) gives a description of the distribution of wave heights in shallow water, based on the output of energy propagation models.

On shallow foreshores waves are subjected to depth-induced breaking. The breaking of particularly the highest waves on shallow foreshores results in a profound change in the shape of the wave height distribution. The distribution of the lower waves in a wave field is still Rayleigh shaped, since the smaller waves propagate relatively undisturbed towards the coast. The distribution of the higher waves deviates considerably from the Rayleigh distribution, since the higher waves in a wave field break. This change in shape of shallow foreshore wave height distributions is not well described by existing local wave height distribution models.

In Chapter 3 a Composed Weibull distribution is proposed to describe the wave height distributions on shallow foreshores. The main feature of the Composed Weibull distribution is the fact that the distribution is composed of two Weibull distributions with different exponents. The domain of the Composed Weibull distribution is split in two by a transitional wave height. This concept was found to yield a good description of observed shallow foreshore wave height distributions.
With empirically estimated values of the two shape parameters and a continuity condition two independent parameters remain. With a physical constraint, relating the mean square wave height to the variance of the surface elevation, the number of independent parameters of the Composed Weibull distribution is limited to one, the transitional wave height. In Chapter 5 forecasting functions for the transitional wave height have been derived. The simplest forecasting function is a breaker criterion where the transitional wave height is directly related to the depth (5.6), yielding a fully predictive, physically based model.

The validation of this Composed Weibull distribution model is carried out in Section 7.4. A new set of measured wave height distributions is compared to wave height distributions computed with the Rayleigh distribution, the New Modified Glukhovskiy distribution and the Composed Weibull distribution model.
The validation proves that the Composed Weibull distribution model yields better approximations of measured wave height distributions than existing distributions on shallow foreshores. The Composed Weibull distribution model as defined in Chapter 7 is simpler and is more physically based than the model defined in Chapter 5.
Therefore it is concluded that the Composed Weibull wave height distribution model, as defined in Chapter 7, is a suitable local wave height distribution model for describing and predicting wave height distributions on shallow foreshores with flat slopes.

Recommendations for further study

Recommendations for further study are the following:

- The main feature of the Composed Weibull distribution is the fact that it contains two different exponents in both parts of the distribution. These exponents are assumed constant and independent of the degree of saturation and the slope of the shallow foreshore. Especially the assumption of a shape factor independent of the bottom slope may possibly decrease the applicability of the Composed Weibull distribution model on steeper foreshores or more complex sloping sea beds. Hence, further investigation is recommended to relate the exponent of the second part of the Composed Weibull distribution to the slope of the foreshore and other parameters of interest.

- The Composed Weibull distribution model, as described in 7.2, does not take the influence of the wave steepness into account. It is recommended to investigate the improvements of the model when the Miche-like forecasting function is used instead of forecasting function (5.6). However, the drawback of using the Miche-like forecasting function is that a third input parameter m_2 is required to obtain the average zero crossing period. This decreases the robustness of the model, as mentioned in Section 5.2.4. Therefore an investigation is recommended of the applicability of an empirical breaker parameter, as mentioned by Battjes and Stive (1985), to take the wave steepness into account

- In this study only laboratory data are used. A validation with prototype data is essential, to investigate the applicability of the Composed Weibull distribution in a complex 3D situation with a non-schematized seabed. For instance, the National Institute for Coastal and Marine Management (RIKZ) executes extensive measurements at the sea-defence works at Petten. A validation of the Composed Weibull distribution model for data obtained in these measurements could yield valuable information.

- When waves break low frequency waves are generated. Low frequency waves influence the wave height distribution, since the water depth is no longer stationary. Hence, an investigation of the influence of low frequency waves on shallow foreshore wave height distributions is recommended.

- Furthermore, it is recommended to investigate the influence of changes in the frequency spectrum of a wave field on the wave height distribution.

Appendix A

Composed Weibull distribution

In Chapter 3 the Composed Weibull distribution is described. In this appendix expressions are derived for the significant wave height $H_{1/3}$ and the ratio of a wave height with a certain probability of exceedance to the significant wave height.

A.1 Mean of the highest 1/N-part

As mentioned in Chapter 3, $H_{1/N}$ is defined by:

$$H_{1/N} = \frac{\int_{H_N}^{\infty} H\, f(H)\,dH}{\int_{H_N}^{\infty} f(H)\,dH} = \frac{\int_{H_N}^{\infty} H\, f(H)\,dH}{\frac{1}{N}\int_{0}^{\infty} f(H)\,dH} = N \int_{H_N}^{\infty} H\, f(H)\,dH \qquad (A.1)$$

In this definition H_N is the wave height with an exceedance probability of $1/N$ (N>1). In coastal engineering practice the wave height with an exceedance probability of $1/N$ is often denoted by $H_{1/N\%}$. However, in this appendix H_N is used instead of $H_{1/N\%}$, in line with the definition of H_N. The determination of $H_{1/N}$ depends on the fact whether or not H_N exceeds H_{tr}.

Transitional wave height exceeds H_N

In Figure A.1 a wave height distribution with H_{tr}> H_N is shown.

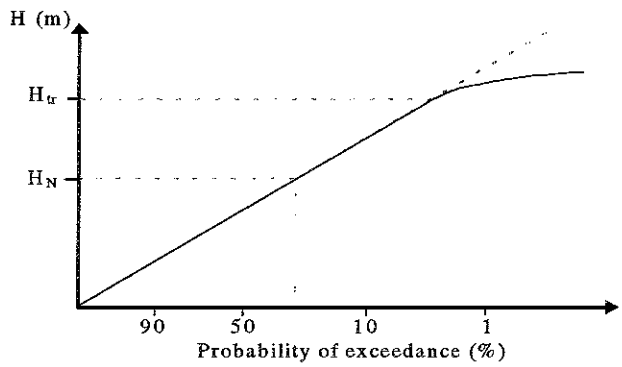

Figure A.1: Composed Weibull wave height distribution with H_{tr}>H_N

In this case H_N is determined by:

$$Q_{\underline{H}_1}(H) \equiv \Pr_1\{\underline{H} \geq H\} = \frac{1}{N} = \exp\left[-\left(\frac{H_N}{H_1}\right)^{k_1}\right] \tag{A.2}$$

Yielding:

$$H_N = H_1[\ln(N)]^{\frac{1}{k_1}} \tag{A.3}$$

$H_{1/N}$ is evaluated via

$$H_{1/N} = N\int_{H_N}^{H_{tr}} H\, f_1(H)\,dH + N\int_{H_{tr}}^{\infty} H\, f_2(H)\,dH \tag{A.4}$$

The first integral can be rewritten into:

$$N\int_{H_N}^{H_{tr}} H\, f_1(H)\,dH = N\int_{H_N}^{\infty} H\, f_1(H)\,dH - N\int_{H_{tr}}^{\infty} H\, f_1(H)\,dH \tag{A.5}$$

yielding:

$$H_{1/N} = N\int_{H_N}^{\infty} H\, f_1(H)\,dH - N\int_{H_{tr}}^{\infty} H\, f_1(H)\,dH + N\int_{H_{tr}}^{\infty} H\, f_2(H)\,dH \tag{A.6}$$

Substitution of the probability density function (3.3) in (A.6) yields:

$$\begin{aligned} H_{1/N} = {} & N\int_{H_N}^{\infty} H\frac{k_1}{H_1^{k_1}} H^{k_1-1}\exp\left[-\left(\frac{H}{H_1}\right)^{k_1}\right]dH - N\int_{H_{tr}}^{\infty} H\frac{k_1}{H_1^{k_1}} H^{k_1-1}\exp\left[-\left(\frac{H}{H_1}\right)^{k_1}\right]dH \\ & + N\int_{H_{tr}}^{\infty} H\frac{k_2}{H_2^{k_2}} H^{k_2-1}\exp\left[-\left(\frac{H}{H_2}\right)^{k_2}\right]dH \end{aligned} \tag{A.7}$$

Assume

$$t = \left(\frac{H}{H_i}\right)^{k_i} \quad \Rightarrow \quad H = H_i\, t^{\frac{1}{k_i}} \quad \Rightarrow \quad dH = \frac{H_i}{k_i}\, t^{\frac{1}{k_i}-1}\, dt \qquad for \quad i = 1,2 \tag{A.8}$$

When this transformation is applied to (A.7) the following equation is obtained:

$$H_{1/N} = NH_1 \int_{\left(\frac{H_N}{H_1}\right)^{k_1}}^{\infty} t^{\frac{1}{k_1}} \exp[-t]dt - NH_1 \int_{\left(\frac{H_{tr}}{H_1}\right)^{k_1}}^{\infty} t^{\frac{1}{k_1}} \exp[-t]dt + NH_2 \int_{\left(\frac{H_{tr}}{H_2}\right)^{k_2}}^{\infty} t^{\frac{1}{k_2}} \exp[-t]dt \quad (A.9)$$

With the incomplete gamma functions described in Section A.4 equation (A.9) is rewritten into :

$$H_{1/N} = NH_1\left(\Gamma\left[\frac{1}{k_1}+1,\ \ln(N)\right]-\Gamma\left[\frac{1}{k_1}+1,\ \left(\frac{H_{tr}}{H_1}\right)^{k_1}\right]\right) + NH_2\Gamma\left[\frac{1}{k_2}+1,\ \left(\frac{H_{tr}}{H_2}\right)^{k_2}\right] \quad (A.10)$$

Transitional wave height exceeded by H_N

Figure A.2 shows a wave height distribution on a shallow foreshore for the case $H_{tr}<H_N$, which means that the transitional wave height is exceeded by the wave height with a certain probability of exceedance, H_N.

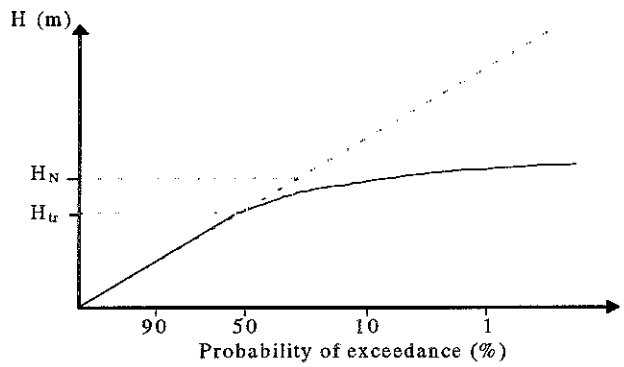

Figure A.2: Composed Weibull wave height distribution with $H_{tr}<H_N$

When H_{tr} is exceeded by H_N, the determination of the $H_{1/N}$ is less complicated. H_N is determined by:

$$Q_{\underline{H}_2} \equiv \Pr_2\{\underline{H} \geq H\} = \frac{1}{N} = \exp\left[-\left(\frac{H_N}{H_2}\right)^{k_2}\right] \quad (A.11)$$

yielding:

$$H_N = H_2[\ln(N)]^{\frac{1}{k_2}} \quad (A.12)$$

$H_{1/N}$ is evaluated via

$$H_{1/N} = N \int_{H_N}^{\infty} H f_2(H) dH \tag{A.13}$$

When the probability density function $f_2(H)$ from the Composed Weibull distribution (3.3) is substituted, the following equation is obtained:

$$H_{1/N} = N \int_{H_N}^{\infty} H \frac{k_2}{H_2^{k_2}} H^{k_2-1} \exp\left[-\left(\frac{H}{H_2}\right)^{k_2}\right] dH \tag{A.14}$$

which can be transformed with (A.8) into:

$$H_{1/N} = N H_2 \int_{\left(\frac{H_N}{H_2}\right)^{k_2}}^{\infty} t^{\frac{1}{k_2}} \exp[-t] dt \tag{A.15}$$

With the incomplete gamma functions (Section A.4) equation (A.15) is rewritten into:

$$H_{1/N} = N H_2 \Gamma\left[\frac{1}{k_2}+1, \left(\frac{H_N}{H_2}\right)^{k_2}\right] \tag{A.16}$$

With (A.12) the following equation is obtained:

$$H_{1/N} = N H_2 \Gamma\left[\frac{1}{k_2}+1, \ln(N)\right] \tag{A.17}$$

In coastal engineering design practice one often is interested in the ratio of an extreme wave height to the significant wave height, $H_{2\%}/H_{1/3}$, $H_{1\%}/H_{1/3}$ or $H_{0.1\%}/H_{1/3}$. The H_N to $H_{1/3}$ ratio for the Composed Weibull distribution is derived in the following section.

A.2 Extreme wave height to significant wave height ratio

In the evaluation of the H_N to $H_{1/3}$ ratio three different situations must be distinguished:

1. $H_N < H_{tr}$
2. $H_3 < H_{tr} < H_N$
3. $H_{tr} < H_3$

with $H_3 < H_N$.

$H_N < H_{tr}$

In relatively deep water the transitional wave height is exceeding both H_3 and H_N, as is shown in Figure A.3. The H_N to $H_{1/3}$ ratio is obtained by evaluating the first part of the composed Weibull distribution $F_1(H)$. The wave height exceeded by 1/N-part of the waves

heights is determined by (A.3) and the significant wave height is determined by equation (A.10).

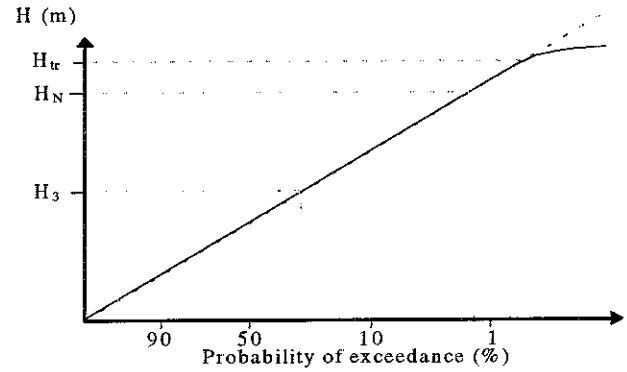

Figure A.3: Composed Weibull wave height distribution with $H_N<H_{tr}$

The H_N to $H_{1/3}$ ratio becomes

$$\frac{H_N}{H_{1/3}} = \frac{H_1\left[\ln(N)\right]^{\frac{1}{k_1}}}{3H_1\left(\Gamma\left[\frac{1}{k_1}+1,\ln(N)\right]-\Gamma\left[\frac{1}{k_1}+1,\left(\frac{H_{tr}}{H_1}\right)^{k_1}\right]\right) + 3H_2\Gamma\left[\frac{1}{k_2}+1,\left(\frac{H_{tr}}{H_2}\right)^{k_2}\right]} \quad \text{(A.18)}$$

$H_3<H_{tr}<H_N$

When the waves propagate into shallower water, the wave height at which the waves deviate from the Rayleigh distribution decreases.

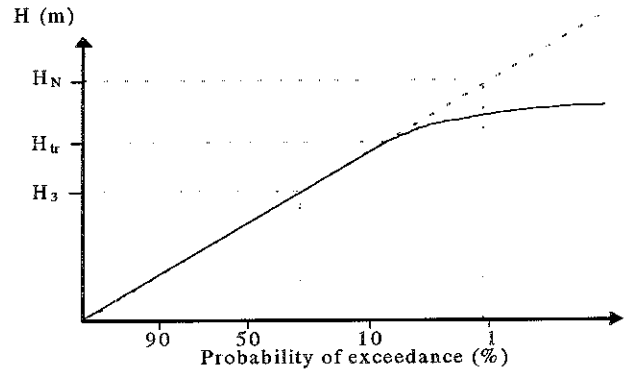

Figure A.4: Composed Weibull wave height distribution with $H_3<H_{tr}<H_N$

As shown in Figure A.4, the transitional wave height is exceeded by the wave height with a probability of exceedance of $1/N$. Therefore H_N is determined by the second part of the composed wave height distribution via equation (A.12). The wave height with an exceedance probability of 1/3, H_3, is now obtained via

$$H_3 = H_1\left[\ln(3)\right]^{\frac{1}{k_1}} \quad \text{(A.19)}$$

when H_3 is smaller than the transitional wave height. Equation (A.10) provides the mean of the highest 1/3-part of the wave height distribution, $H_{1/3}$. Thus, for $H_3 < H_{tr} < H_N$ the following equation determines the H_N to $H_{1/3}$ ratio:

$$\frac{H_N}{H_{1/3}} = \frac{H_2\left[\ln(N)\right]^{\frac{1}{k_2}}}{3H_1\left(\Gamma\left[\frac{1}{k_1}+1,\ \ln(3)\right]-\Gamma\left[\frac{1}{k_1}+1,\ \left(\frac{H_{tr}}{H_1}\right)^{k_1}\right]\right) + 3H_2\Gamma\left[\frac{1}{k_2}+1,\ \left(\frac{H_{tr}}{H_2}\right)^{k_2}\right]} \quad \text{(A.20)}$$

$H_{tr} < H_3$

In Figure A.5 the wave height, with an exceedance probability of 1/3, H_3, exceeds the transitional wave height.

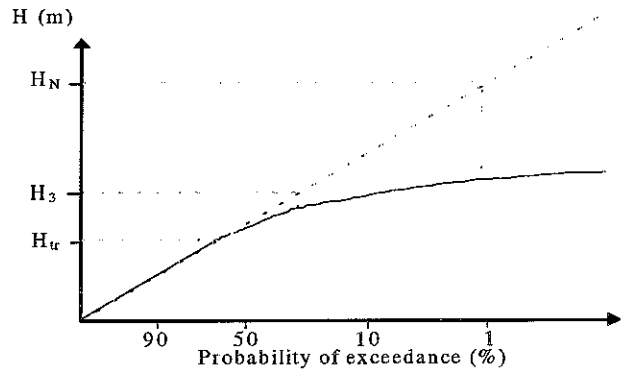

Figure 3.5: Composed Weibull height distribution with $H_{tr} < H_3$.

All wave heights exceeding H_{tr} obey the second part of the wave height distribution, $F_2(H)$, H_N is determined by (A.12) and the significant wave height by

$$H_{1/3} = 3\,H_2\,\Gamma\left[\frac{1}{k_2}+1,\ \ln(3)\right] \quad \text{(A.21)}$$

Therefore the following H_N to $H_{1/3}$ ratio is found:

$$\frac{H_N}{H_{1/3}} = \frac{\left[\ln(N)\right]^{\frac{1}{k_2}}}{3\Gamma\left[\frac{1}{k_2}+1,\ \ln(3)\right]} \quad \text{(A.22)}$$

A.3 Evaluation of the $H_{1\%}$ to $H_{1/3}$ ratio

In this section a specific ratio of a wave height with a certain probability of exceedance to the significant wave height is evaluated as an example. Since in coastal engineering practice $H_{1/N\%}$ is often used to represent a wave height with a certain probability of exceedance, in this section the same notation is used.

$H_{1\%}$ to $H_{1/3}$ ratio in deep water

In this section the $H_{1\%}$ to $H_{1/3}$ ratio is given for deep and extremely shallow water. In deep water, where all the wave heights obey the Rayleigh distribution $H_{tr} \rightarrow \infty$. This means that (A.18) reduces to

$$\lim_{H_{tr}\rightarrow\infty}\left(\frac{H_N}{H_{1/3}}\right) = \frac{[\ln(N)]^{\frac{1}{k_1}}}{3\Gamma\left[\frac{1}{k_1}+1,\ \ln(3)\right]} \qquad \text{(A.23)}$$

In Section 3.3.2 assumptions are proposed for the exponents k_1 and k_2, i.e $k_1=2$ and $k_2=3.5$. If $k_1=2$ and $N=100$ are substituted in equation (A.23), the following $H_{1\%}$ to $H_{1/3}$ ratio is obtained:

$$\frac{H_{1\%}}{H_{1/3}} = \frac{[\ln(100)]^{\frac{1}{2}}}{3\Gamma\left[\frac{1}{2}+1,\ \ln(3)\right]} \approx 1.52 \qquad \text{(A.24)}$$

This is in line with the $H_{1\%}$ to $H_{1/3}$ ratio of the Rayleigh distribution, since from (2.4):

$$Q_{\underline{H}}(H) \equiv \Pr\{\underline{H} > H\} = \exp\left[-2\left(\frac{H}{H_{1/3}}\right)^2\right] \qquad \text{(A.25)}$$

the same $H_{1\%}$ to $H_{1/3}$ ratio is obtained:

$$\frac{H_{1\%}}{H_{1/3}} = \sqrt{\tfrac{1}{2}\ln\left(Q_H^{-1}\right)} = \sqrt{\tfrac{1}{2}\ln(100)} \approx 1.52 \qquad \text{(A.26)}$$

$H_{1\%}$ to $H_{1/3}$ ratio in extremely shallow water

In extremely shallow water, where $H_{1\%}$ and H_3 exceed the transitional wave height, equation (A.22) was found to represent the $H_{1\%}$ to $H_{1/3}$ ratio. When k_2= 3.5 is substituted in (A.22) the following constant $H_{1\%}$ to $H_{1/3}$ ratio is obtained:

$$\frac{H_{1\%}}{H_{1/3}} = \frac{[\ln(100)]^{\frac{1}{3.5}}}{3\Gamma\left[\frac{1}{3.5}+1,\ \ln(3)\right]} \approx 1.28 \qquad \text{(A.27)}$$

This means that, when $H_{tr} < H_3$, the H_N to $H_{1/3}$ ratio fully depends on the shape of the second part of the composed wave height distribution.

A.4 Incomplete gamma functions

The gamma function is defined by:

$$\Gamma(a) = \int_0^\infty t^{a-1}\exp[-t]\,dt \qquad 0 < t < \infty \qquad \text{(A.28)}$$

This gamma function is a generalization of the factorial function. The gamma function has the following properties.

$$\Gamma(a+1) = a\Gamma(a) \tag{A.29}$$

$$\Gamma(a+1) = a! \qquad for \quad a=1,2,\ldots,n \tag{A.30}$$

The incomplete gamma function is defined by (Abramowitz and stegun 1965):

$$P(a,x) = \frac{\gamma(a,x)}{\Gamma(a)} = \frac{1}{\Gamma(a)}\int_0^x t^{a-1}\exp[-t]\,dt \qquad (a>0) \tag{A.31}$$

in which Γ(a) is the complete gamma function. Therefore $\gamma(a,x)$ is defined by:

$$\gamma(a,x) = \int_0^x t^{a-1}\exp[-t]\,dt \tag{A.32}$$

The complement of $P(a,x)$ is defined by:

$$Q(a,x) = 1-P(a,x) = \frac{\Gamma(a,x)}{\Gamma(a)} = \frac{1}{\Gamma(a)}\int_x^\infty t^{a-1}\exp[-t]\,dt \tag{A.33}$$

yielding

$$\Gamma(a,x) = \int_x^\infty t^{a-1}\exp[-t]\,dt \tag{A.34}$$

Appendix B

Shallow foreshore test set-up

In Section 4.1 the available foreshore data are described. In this appendix, the test set-up of the data presented in Table 4.1 are shown.

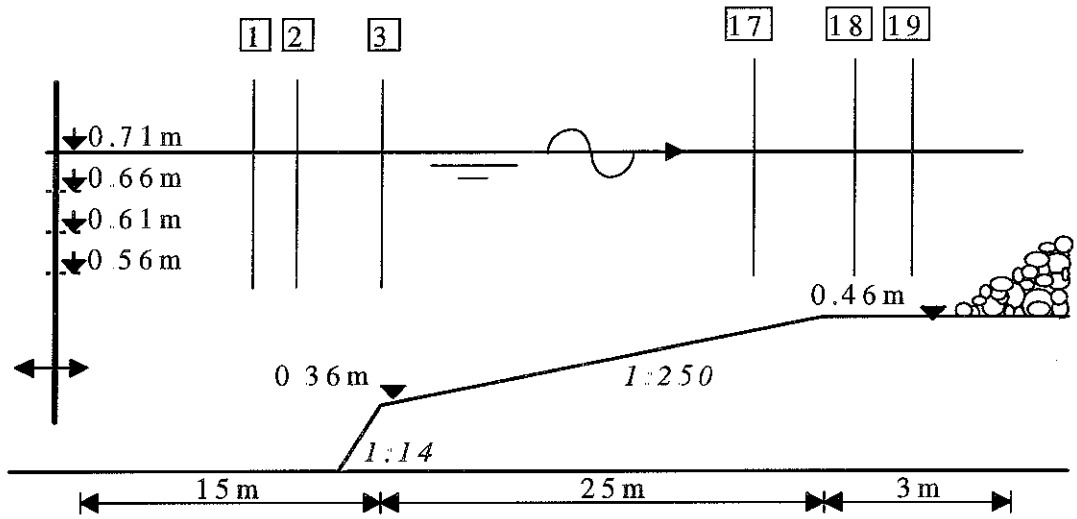

Figure B.1: Shallow foreshore test set-up, slope 1:250, H0462-25.

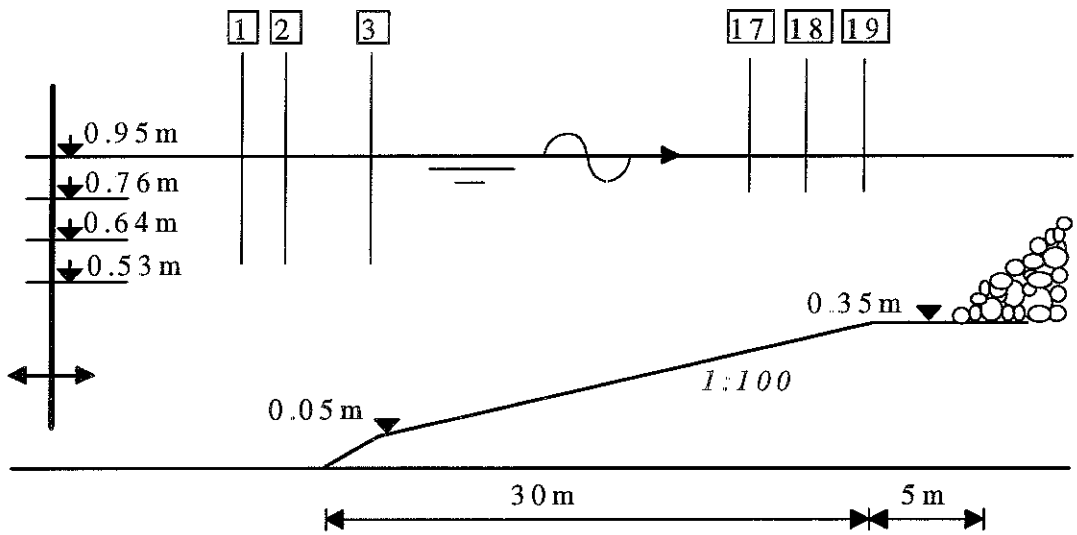

Figure B.2: Shallow foreshore test set-up, slope 1:100, H1256.

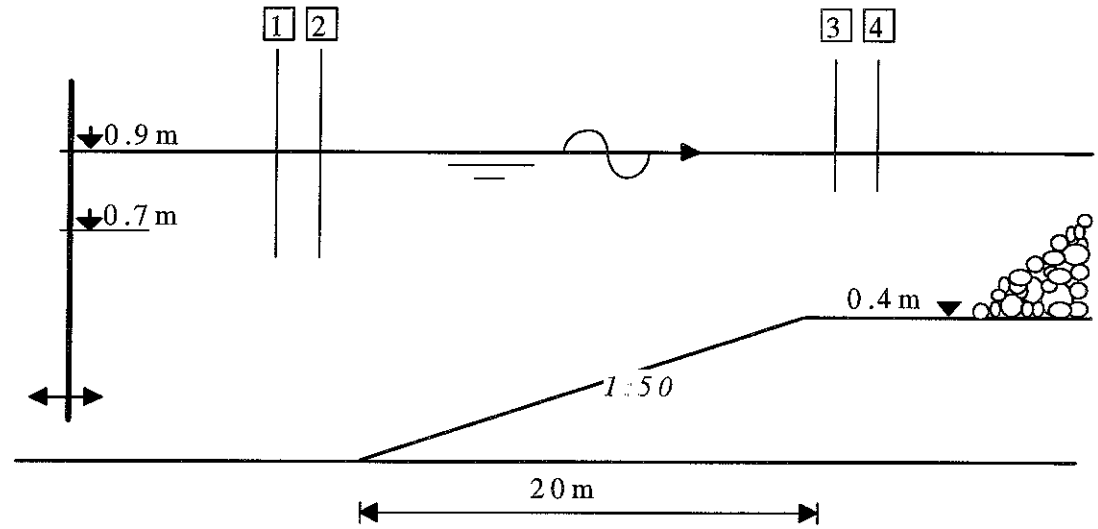

Figure B.3: Shallow foreshore test set-up, slope 1:50, H1874-50

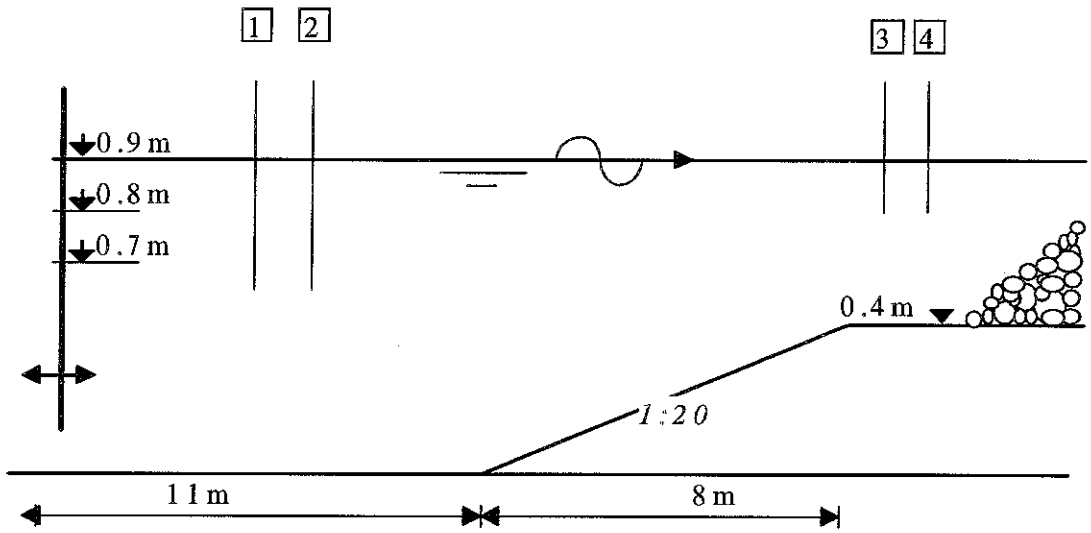

Figure B.4: Shallow foreshore test set-up, slope 1:20, H1850-09.

Appendix C

Table 7.1: Characteristic nondimensional wave heights $\tilde{H}_x$ as function of $\tilde{H}_{tr}$

$\tilde{H}_{tr}$	$\tilde{H}_1$	$\tilde{H}_2$	$\tilde{H}_{1/3}$	$\tilde{H}_{1/10}$	$\tilde{H}_{2\%}$	$\tilde{H}_{1\%}$	$\tilde{H}_{0.1\%}$
0.05	10.466	1.060	1.286	1.480	1.565	1.639	1.841
0.10	6.223	1.060	1.286	1.480	1.565	1.639	1.841
0.15	4.591	1.060	1.286	1.480	1.565	1.639	1.841
0.20	3.700	1.060	1.286	1.480	1.565	1.639	1.841
0.25	3.130	1.060	1.286	1.480	1.565	1.639	1.841
0.30	2.730	1.060	1.286	1.480	1.565	1.639	1.841
0.35	2.433	1.060	1.286	1.480	1.565	1.640	1.841
0.40	2.202	1.060	1.286	1.480	1.565	1.640	1.841
0.45	2.017	1.060	1.287	1.481	1.566	1.640	1.842
0.50	1.865	1.061	1.287	1.482	1.566	1.641	1.843
0.55	1.739	1.062	1.288	1.483	1.568	1.643	1.844
0.60	1.632	1.063	1.290	1.484	1.570	1.644	1.846
0.65	1.541	1.065	1.292	1.487	1.572	1.647	1.849
0.70	1.464	1.067	1.295	1.490	1.576	1.651	1.853
0.75	1.397	1.070	1.299	1.494	1.580	1.655	1.859
0.80	1.339	1.074	1.303	1.500	1.586	1.661	1.865
0.85	1.289	1.079	1.309	1.506	1.593	1.669	1.874
0.90	1.247	1.084	1.316	1.514	1.601	1.677	1.883
0.95	1.210	1.091	1.324	1.523	1.611	1.687	1.895
1.00	1.178	1.098	1.333	1.534	1.622	1.699	1.908
1.05	1.151	1.107	1.343	1.545	1.634	1.712	1.922
1.10	1.128	1.116	1.354	1.558	1.648	1.726	1.938
1.15	1.108	1.126	1.366	1.572	1.663	1.742	1.956
1.20	1.091	1.137	1.378	1.587	1.678	1.758	1.974
1.25	1.077	1.148	1.387	1.603	1.695	1.776	1.994
1.30	1.065	1.160	1.395	1.620	1.713	1.794	2.015
1.35	1.054	1.172	1.400	1.637	1.731	1.814	2.036
1.40	1.046	1.185	1.405	1.655	1.750	1.833	2.058
1.45	1.038	1.198	1.408	1.673	1.769	1.853	2.081
1.50	1.032	1.211	1.410	1.692	1.789	1.874	2.104
1.55	1.027	1.225	1.412	1.711	1.809	1.895	2.128
1.60	1.022	1.239	1.414	1.728	1.829	1.916	2.151
1.65	1.018	1.252	1.415	1.742	1.849	1.937	2.175
1.70	1.015	1.266	1.415	1.754	1.870	1.959	2.199
1.75	1.013	1.280	1.416	1.763	1.890	1.980	2.224
1.80	1.010	1.294	1.416	1.771	1.911	2.002	2.248
1.85	1.008	1.308	1.416	1.777	1.931	2.023	2.272
1.90	1.007	1.322	1.416	1.782	1.952	2.045	2.296
1.95	1.006	1.336	1.416	1.786	1.972	2.066	2.320
2.00	1.005	1.349	1.416	1.789	1.987	2.088	2.344
2.05	1.004	1.363	1.416	1.791	1.985	2.109	2.368
2.10	1.003	1.377	1.416	1.793	1.984	2.130	2.391
2.15	1.002	1.390	1.416	1.795	1.983	2.151	2.415

$\tilde{H}_{tr}$	$\tilde{H}_1$	$\tilde{H}_2$	$\tilde{H}_{1/3}$	$\tilde{H}_{1/10}$	$\tilde{H}_{2\%}$	$\tilde{H}_{1\%}$	$\tilde{H}_{0.1\%}$
2.20	1.002	1.404	1.416	1.796	1.982	2.150	2.438
2.25	1.002	1.417	1.416	1.797	1.981	2.149	2.461
2.30	1.001	1.430	1.416	1.798	1.980	2.149	2.484
2.35	1.001	1.443	1.416	1.798	1.980	2.148	2.507
2.40	1.001	1.456	1.416	1.799	1.979	2.148	2.529
2.45	1.001	1.469	1.416	1.799	1.979	2.147	2.551
2.50	1.000	1.481	1.416	1.799	1.979	2.147	2.573
2.55	1.000	1.494	1.416	1.799	1.979	2.147	2.595
2.60	1.000	1.506	1.416	1.799	1.978	2.147	2.617
2.65	1.000	1.519	1.416	1.800	1.978	2.146	2.629
2.70	1.000	1.531	1.416	1.800	1.978	2.146	2.629
2.75	1.000	1.543	1.416	1.800	1.978	2.146	2.629
2.80	1.000	1.555	1.416	1.800	1.978	2.146	2.629
2.85	1.000	1.567	1.416	1.800	1.978	2.146	2.628
2.90	1.000	1.578	1.416	1.800	1.978	2.146	2.628
2.95	1.000	1.590	1.416	1.800	1.978	2.146	2.628
3.00	1.000	1.601	1.416	1.800	1.978	2.146	2.628
3.05	1.000	1.613	1.416	1.800	1.978	2.146	2.628
3.10	1.000	1.624	1.416	1.800	1.978	2.146	2.628
3.15	1.000	1.635	1.416	1.800	1.978	2.146	2.628
3.20	1.000	1.646	1.416	1.800	1.978	2.146	2.628
3.25	1.000	1.657	1.416	1.800	1.978	2.146	2.628
3.30	1.000	1.668	1.416	1.800	1.978	2.146	2.628
3.35	1.000	1.679	1.416	1.800	1.978	2.146	2.628
3.40	1.000	1.690	1.416	1.800	1.978	2.146	2.628
3.45	1.000	1.700	1.416	1.800	1.978	2.146	2.628
3.50	1.000	1.711	1.416	1.800	1.978	2.146	2.628

References

Battjes, J.A. (1974): *Computation of set-up, longshore currents, run-up and overtopping due to wind-generated waves*, Delft University of Technology, Department of Civil Engineering, Section Fluid Mechanics, The Netherlands.

Battjes, J.A. and J.P.F.M. Janssen (1978): Energy loss and set-up due to breaking of random waves, in *Proceedings of the 16th International Conference on Coastal engineering*, pp. 569-587, American Society of Civil Engineers, New York.

Battjes, J.A. and M.J.F. Stive (1985): Calibration and Verification of a Dissipation Model for Random Breaking Waves, *J. Geophys. Res., 90*, pp. 9159-9167.

Battjes, J.A. (1994): Shallow water wave modelling, in *Proceedings of the international symposium: Waves, physical and numerical modelling*, pp. 1-23, University of British Columbia, Vancouver, Canada.

Van Epen, D. (1990): *Golfhoogtes van brekende golven op een flauw talud*, H462, Delft Hydraulics, The Netherlands.

Gerding, E. (1993): *Toe stability of rubble mound breakwaters*, H1874, Delft Hydraulics, The Netherlands.

Horikawa, K. (1988): *Nearshore dynamics and coastal processes*, University of Tokyo Press, Tokyo.

Klopman, G and M.J.F. Stive (1989): *Extreme waves and wave loading in shallow water*, paper presented at the E&P Forum Workshop in Paris, Delft Hydraulics, The Netherlands.

Klopman, G. (1995): *Golfhoogten op ondiep water*, project voorstel H2036 , Delft Hydraulics, The Netherlands.

Klopman, G. (1996): *Extreme wave heights in shallow water*, H2486, Delft Hydraulics, The Netherlands.

Longuet-Higgins, M.S. (1952): On the statistical distributions of heights of sea waves, *J. of Mar. Res.*, Vol. XI, pp. 245-266.

Longuet-Higgins, M.S (1957): The statistical analysis of a random, moving surface, *Phil. Trans Roy. Soc. London*, Vol. 249, pp. 321 -387.

Longuet-Higgins, M.S. (1975): On the joint distribution of the periods and amplitudes of sea waves, *J. Geophys. Res., 80*, pp. 2688-2694.

Longuet-Higgins, M.S. (1980): On the distribution of the heights of sea waves: Some effects of nonlinearity and finite band width, *J. Geophys. Res., 85*, pp. 1519-1523.

Van der Meer, J.W. (1997): *Golfoploop en overslag bij dijken*, H2458/3051, Delft Hydraulics, The Netherlands.

Ochi, M.K. (1990): *Applied Probability and Stochastic progresses*, University of Florida, Wiley Interscience, USA.

Pollard, A. and C. Rivoire (1971): *Fiabilité et Statistiques, La Méthode de Weibull*, Étudions Eyrolles et Étudions d'Organisation, Paris, France.

Pilarczyk, K.W. (1996): *Inleiding op de bijeenkomst: "Ondiepe voorlanden"*, Delft, The Netherlands.

Rice, S.O. (1954): Mathematical analysis of random noise, 1944, reprinted in *Selected paper on Noise and Stochastic Processes*, Dover Pub. inc., pp. 133-294.

Stive, M.J.F. (1986): *Extreme shallow water wave conditions*, H533, Delft Hydraulics, The Netherlands.

Tayfun, M.A. (1990): Distribution of large wave heights, *J. Waterway, Port, Coastal and Ocean Engng. 116(6)*, pp. 686-707.

Van Vledder, G. Ph. (1993): *Note 43: Split Weibull distribution, version 2.0*, Delft Hydraulics, The Netherlands

Van Vledder, G. Ph. (1997): *Personal communication*.

Notation

Roman letters:

A	:	parameter based on the exponent in the Glukhovskiy distribution (-)
d	:	water depth (m)
d_t	:	water depth at the toe of the sea-defence work (m)
$\tilde{d}$	:	ratio of mean wave height to water depth, H_m/d (-)
d^*	:	ratio of root mean square wave height to water depth, H_{rms}/d (-)
H	:	wave height (m)
H_i	:	scale wave height of the Composed Weibull distribution (m)
$H_{1/3}$	:	significant wave height defined as the mean of the highest 1/3-part of the wave heights in a wave field (m)
$H_{1/3,0}$	:	incident significant wave height (m)
$H_{1/3,t}$	:	significant wave height at the toe of the sea-defence work (m)
H_m	:	mean wave height (m)
H_{m0}	:	spectral significant wave height, $H_{m0} = 4\sqrt{m_0}$ (m)
H_N	:	the wave height with an exceedance probability of $1/N$ (m)
$H_{1/N}$	:	mean of the highest $1/N$-part of the wave heights in a wave field (m)
H_{rms}	:	root mean square wave height (m)
H_t	:	transition wave height of the split Weibull distribution (Van Vledder 1993) (m)
H_{tr}	:	transitional wave height of the Composed Weibull distribution (m)
$\tilde{H}_x$	:	nondimensionalized characteristic wave height, $\tilde{H}_x = H_x/H_{rms}$ (-)
k_i	:	exponent of the Composed Weibull distribution (-)
L_f	:	foreshore length (m)
L_{op}	:	deep water wavelength based on the peak period T_p (m)
L_{02}	:	local wave length based on the average zero-crossing period T_{02} (m)
m_n	:	n^{th} moment of the frequency spectrum (m^2)
m_0	:	variance of the water surface elevation, i.e. the total wave energy (m^2)
T_{02}	:	average zero-crossing period, $T_{02} = \sqrt{m_0/m_2}$ (s)

Greek letters:

α	:	slope of the foreshore (-)
α_{H1}	:	empirical coefficient of the scale wave height forecasting function (-)
α_{tr}	:	empirical coefficient of the transitional wave height forecasting function (-)
β	:	coefficient of the Modified Glukhovskiy distribution (Klopman 1996) (-)
β_{tr}	:	empirical coefficient of the transitional wave height forecasting function (-)
ε_{rms}	:	root mean square error (-)
γ_{tr}	:	empirical breaker coefficient of the transitional wave height (-)
κ	:	exponent of the Glukhovskiy distribution (-)
κ^*	:	exponent of the Modified Glukhovskiy distribution (Klopman 1996) (-)
σ	:	scale wave height of the split Weibull distribution (Van Vledder 1993) (m)
Ψ	:	degree of saturation, $\Psi = \sqrt{m_0}/d$ (-)